**RESEARCH PAPER**

# Polymer-Engineered Pulsatile Matrix Tablets of Carvedilol: Optimization, Release Kinetics, and Mechanistic Insights into Chronomodulated Drug Delivery

**Raja Majumder[1], Aritra Ghosh[1], Abhishek Mandal[1], Arunima Nag[1], AnneshaChakraborty[1], Arnab Mukherjee[1], Trisha Chatterjee[1], Dishari Dutta[1], Krishnendu Sahoo[2]**

[1]*Bengal School of Technology, Delhi-Road, Sugandha, Hooghly, West Bengal, India, 712102*

[2]*Bengal College of Pharmaceutical Technology, Dubrajpur, Birbhum, West Bengal, 731123*

***Received: 13May, 2026; Revised: 12th Jun, 2026; Accepted: 25th Jun, 2026; Available Online: 20July, 2026***

**ABSTRACT**

Pulsatile-release delivery systems have gained prominence in pharmaceutical development as alternatives to conventional controlled-release methods, which are often limited by continuous drug delivery profiles. In this study, carvedilol was used as an API to evaluate the efficacy of matrix tablets formulated with a blend of **HPMC** K100 and **Ethyl cellulose**. ***The investigation identified formulations F5 and F9 as optimal, as they achieved the desired lag-time pattern with a delay exceeding 6 hours***. According to the Korsmeyer-Peppas model, the adjusted $R^2$ values for formulations F5 and F9 were 0.99, indicating a high degree of fit. Analysis via DD-Solver yielded Akaike Information Criterion values of 39.37 and 33.71, alongside Model Selection Criterion values of 4.51 and 4.93 for F5 and F9, respectively. The drug release profile from the polymeric matrix was characterized by non-Fickian and Super Case-II transport mechanisms, with an exponent 'n' value exceeding 1. ***Findings indicate that while ethyl cellulose inhibits drug release, HPMC facilitates it***. Post hoc Tukey-HSD analysis revealed that the optimized formulations F2, F5, and F9 exhibited no significant differences in release at $t_{10\%}$, followed by accelerated release profiles after $t_{50\%}$ **and** $t_{80\%}$. ***Notably, formulation F5 sustained the desired release retardation up to 6 hours (24% release)***, whereas F2 and F9 demonstrated higher release rates (45-50%). Given that F9 exhibited a prolonged release profile, F5 was identified as the optimal formulation for maintaining the desired pulsatile release. This performance aligns with the requirements for chronomodulated therapy, where the structural integrity of the coating prevents premature dissolution while allowing for rapid drug liberation upon the onset of symptoms.

**Keywords:** Pulsatile Drug Delivery, Kinetic Study, HPMC, Ethyl cellulose

**How to cite this article:** Raja Majumder, Aritra Ghosh, Abhishek Mandal, Arunima Nag, AnneshaChakraborty, Arnab Mukherjee, Trisha Chatterjee, Dishari Dutta, Krishnendu Sahoo, Polymer-Engineered Pulsatile Matrix Tablets of Carvedilol: Optimization, Release Kinetics, and Mechanistic Insights into Chronomodulated Drug Delivery. Int J Drug Deliv Technol. 2026;16(73s): 198-220. DOI: 10.25258/ijddt.16.73s.20

**Source of support:** Nil.

**Conflict of interest:** None

## INTRODUCTION

Among other drug delivery systems, pulsatile delivery stands out to its innovative design, which makes it a cutting-edge method of creating chronotherapy that is tailored to the condition and the medicine's characteristics. By adjusting the time of drug administration, which may affect the pharmacokinetic characteristics of medications, chronotherapy is the adaptation of medicine to biological rhythm to achieve maximum efficacy. The science of chronopharmacology focuses on maximizing the effects of drugs and minimizing their side effects by adjusting dosage timing according to biological rhythms, which are time-related periodic phenomena in living things. These rhythms are classified as **Circadian** (*the oscillation is finished in 24 hours*), **Ultradian** (*the oscillation is finished in less than 24 hours*), and **Infradian** (*the oscillations are longer than 24 hours*)[1–3].

Hypertension, a significant risk factor for cardiovascular disease (CVD), is characterized by a consistent systolic and diastolic blood pressure of 140/90mmHg or above. This chronic elevation of blood pressure can lead to severe complications and potentially fatal events. ***Circadian variation in hypertension contributes to the increase in acute cardiovascular events in the early morning hours***[4,5]. Blood pressure (BP) in both normal and hypertensive individuals varies during the day, with higher heart rates and blood pressure during the early morning. This is due to a decrease in sympathetic output at bedtime, leading to a rapid rise in systolic and diastolic blood pressure. In cardiovascular disease (CVD), capillary resistance and vascular reactivity are higher in the early morning, leading to increased platelet aggregation and decreased fibrinolytic activity [6–8]. This increases the risk of myocardial ischemia, acute myocardial infarction, angina pectoris, cardiac failure, and sudden cardiac arrest. Ambulatory blood pressure monitoring (*ABPM*) has been introduced into regular hypertension management to observe day-night patterns of blood pressure. An exaggerated morning blood pressure surge (MBPS) is closely related to increased risk of cardiovascular diseases and all-cause mortality [9–11].

**Author for Correspondence:* Raja Majumder

***Hermida et al.*** conducted a study on the impact of antihypertensive drugs and treatment time on blood pressure in 585 hypertensive patients with diabetes mellitus. They found that blood pressure was reduced during diurnally active hours but not during night-time sleep, indicating the importance of a proper chronotherapeutic scheme to reduce blood pressure and modify the distorted circadian profile [12,13]. ***Konga et al.*** conducted a chronotherapeutic test with ***β-blockers*** to prevent the ***morning escalation of hypertension*** with an ***evening dose of carvedilol***. The results showed that the morning surge in BP was suppressed and 24-hour mean systolic pressure was also reduced with carvedilol [14,15]. ***Hermida et al.*** concluded that bedtime administration of antihypertensive medications significantly improved blood pressure control and reduced the occurrence of major cardiovascular events [16].

Chronotherapeutics is the purposeful alteration of drug levels to match rhythms to optimize therapeutic outcomes and minimize side effects. One should not assume that a drug dosed in the morning will have the same antihypertensive effect as a drug dosed in the evening. ***Novel drug delivery systems have the potential to provide antihypertensive medication at the time when the need is greatest***. For the treatment of hypertension, this idea has the potential for a therapeutic paradigm shift. To prevent these events, chronotherapeutics can be used in hypertensive management. Pulsatile drug delivery technologies, designed to regulate biological clocks, release drugs in pulses only after a lag time. These technologies help regulate biochemical and physiological activities, such as the sleep-wake cycle, hormone secretion, body temperature, and blood pressure [17–21].

Employing the press-coating approach to alter drug release profiles and accomplish certain release patterns, press-coating technology produces tablets with controlled drug release and programmed lag periods. This method enables the production of press-coated tablets with various release profiles by compaction of a dry-coat around a tablet core. ***Compared to traditional dose forms, pulsatile drug delivery systems offer more benefits by delivering the medication at the appropriate time, location, and dosage***. By maximizing therapeutic efficacy and reducing adverse effects, these systems improve patient compliance [22–24]. These methods enable adjustable medication release patterns to fulfil unique therapeutic demands by promising a predefined lag period followed by quick drug release. Press coating procedures frequently include pharmaceutical polymers, including wax, methacrylate copolymers, polysaccharides, cellulose derivatives, and water-soluble polymers. Water insoluble/rupturable (*EC*), erodible (*low molecular weight HPMC, HPC, PEO*), gellable or swellable (*high molecular weight HPMC, gums*), pH-dependent soluble (*HPMCAS, Eudragit copolymers*), waxy, and bacterially digested are some of the classes into which these polymers may be divided [25–29]. Press-coated tablet medication release behaviour may be controlled and modulated by the kind and molecular weight of the polymer used to produce the outer coating shell. Drug release from the inner core is inhibited by a purely erodible covering until the dissolving media removes it. The performance of press-coated tablet release, however, can be delayed and changed by a gellable coating. In this project, the design was to ***maximize*** the ***desired lag-time*** and maintain sustainable release after lag-time;***CARVEDILOL***(a *non-cardioselective beta-blocker)* that is used to treat ***hypertension*** and ***angina pectoris***, was incorporated as an API in a ***core tablet with a combination of ethylcellulose (EC) and hydroxypropyl methylcellulose (HPMC) as an outer layer*** to intervene the press-coating [30,31]. It's a combination of erodible and swellable properties at different concentrations. This formulation strategy leverages the distinct erosion characteristics of hydroxypropyl methylcellulose alongside the hydrophobic barrier properties of ethylcellulose to precisely modulate the onset of drug release [32].

## MATERIALS AND METHODS

### Materials

**Carvedilol**, a non-selective α- and β-adrenergic receptor antagonist (*molecular formula: $C_{24}H_{26}N_2O_4$; molecular weight: 406.47 g/mol*), was selected as the model antihypertensive drug for the development of a chronotherapeutic pulsatile press-coated tablet. The active pharmaceutical ingredient (API) was kindly supplied as a ***gift sample by CTX Lifesciences Pvt. Ltd., Surat, India. β-Cyclodextrin*** (*Yarrow Chem Products, Mumbai, India*) was employed as the inclusion complexing agent to enhance drug solubility. Mannitol (*Research-Lab Fine Chem Industries, Mumbai, India*) was used as the diluent, while microcrystalline cellulose (*LobaChemiePvt. Ltd., Mumbai, India*) served as the filler and binder. Croscarmellose sodium (Thermo Fisher Scientific India Pvt. Ltd., Mumbai, India) and sodium starch glycolate (*LobaChemiePvt. Ltd., Mumbai, India*) were incorporated as superdisintegrants in the core tablet formulation. Talc and magnesium stearate (*LobaChemiePvt. Ltd., Mumbai, India*) were used as the glidant and lubricant, respectively. Hydroxypropyl methylcellulose (*HPMC K100; Evonik Röhm GmbH, Germany*) and ethyl cellulose (*Sisco Research Laboratories Pvt. Ltd., Mumbai, India*) were utilized as the hydrophilic and hydrophobic polymers, respectively, for the press-coating layer to achieve the desired lag time and pulsatile drug release. All chemicals and reagents used in the study were of analytical reagent (AR) grade and were used without further purification.

### Instrumentation

The formulation and characterization studies were performed using standard pharmaceutical laboratory equipment. An electronic analytical balance (*Wensar Weighing Scales Ltd., Chennai, India*) was used for

accurate weighing of materials. Powder blending was carried out using a rotary shaker (*Labtech Instruments, India*) and vortex mixer (*Rawal Scientific Glass Works, India*), while an ultrasonicator bath (*IKON Industries, India*) was employed for sample homogenization. Drying operations were performed in a hot air oven (*R. S. Scientific, West Bengal, India*). Tablet compression was accomplished using a rotary tablet compression machine (*Lodha International LLP, India*). Pre-compression and post-compression quality control parameters were evaluated using a bulk density apparatus (*Analab Scientific Instruments, India*), Monsanto hardness tester (USA), friability tester (*Analab Scientific Instruments, India*), and micrometer screw gauge (*H. L. Scientific Industries, India*). Drug content estimation and in vitro dissolution studies were carried out using a UV–Visible spectrophotometer (*Pnaomex Inc., India*) and a USP dissolution test apparatus (*Labindia Analytical Instruments Pvt. Ltd., India*), respectively. The pH of the formulations was measured using a digital pH meter (*Digital Instruments Corp., Gujarat, India*). Fourier Transform Infrared spectroscopy equipped with an Attenuated Total Reflectance (*ATR-FTIR*) accessory (*Specac, UK*) was employed to investigate possible drug–excipient interactions, and Whatman filter paper (*Cytiva, USA*) was used for filtration during analytical procedures.

**Analytical Characterization of Carvedilol**

Before formulation development, Carvedilol was subjected to physicochemical and analytical characterization. Phosphate buffer (pH 6.8) and 0.1 N hydrochloric acid (HCl) were prepared according to standard pharmacopeial procedures and used as dissolution and analytical media. A primary stock solution of Carvedilol was prepared by dissolving 50 mg of the drug in methanol, followed by appropriate dilution with 0.1 N HCl or phosphate buffer (pH 6.8) to obtain the required working concentrations [33,34]. The absorption spectrum of Carvedilol was recorded using a UV–Visible spectrophotometer over an appropriate wavelength range, and the maximum absorption wavelength (λmax) was identified at 241 nm. A calibration curve was subsequently constructed by preparing serial dilutions of the stock solution, and absorbance was measured at 241 nm in accordance with the Beer–Lambert law to establish linearity for quantitative drug estimation. The melting point of Carvedilol was determined using the capillary method to verify its identity and purity. Drug–excipient compatibility was evaluated by Attenuated Total Reflectance–Fourier Transform Infrared (ATR–FTIR) spectroscopy, wherein spectra of the pure drug, individual excipients, and their physical mixtures were recorded over the characteristic infrared region to identify functional groups and detect any potential chemical interactions. The pre-compression characteristics of the powder blends were evaluated by determining bulk density, tapped density, Hausner's ratio, Carr's compressibility index, and angle of repose using standard pharmacopeial methods [35–37]. These micromeritic parameters were assessed to determine the flowability, compressibility, and suitability of the powder blends for direct compression during the preparation of the pulsatile press-coated tablets.

**Preparation of the Carvedilol and β-Cyclodextrin complex**

The Carvedilol–β-Cyclodextrin complex was prepared using the kneading technique, a well-established method for enhancing drug solubility. Initially, Carvedilol and β-Cyclodextrin were accurately weighed in a 1:3 weight ratio and blended thoroughly using a mortar and pestle. The mixture was then moistened with an ethanol–water solvent system (15:85 v/v) and ground continuously to form a consistent paste. To ensure optimal complexation, the remaining solvent was added dropwise to the paste over approximately 45 minutes under constant, steady grinding. Subsequently, the resulting paste was left to dry naturally at room temperature overnight. Once fully dried, the solid mass was pulverized and passed through a number 120 mesh sieve. The final complex was stored securely in an airtight container at room temperature to preserve its stability and properties for further pharmaceutical applications [38–41].

**Preparation of Fast-Dissolving Core Tablet:**

The fast-dissolving core tablet was meticulously prepared using the direct compression method, focusing on the precise formulation outlined in the table for 6.25 mg carvedilol. To enhance disintegration, Sodium starch glycolate (SSG) was incorporated as a superdisintegrant; microcrystalline cellulose (MCC) acted as a binder; mannitol served as a diluent; and Magnesium stearate and talc were added as a lubricant and glidant, respectively, ensuring optimal flow properties of the powdered mixture. All ingredients, including the carvedilol-β-Cyclodextrin complex, underwent meticulous sieving through a number 60 sieve before being accurately weighed in accordance with the formulation table. Subsequently, a thorough 30-minute mixing period was observed to guarantee homogeneous distribution of the drug particles.Following this, the blend was enriched with talc and Magnesium stearate before undergoing a comprehensive evaluation of key preformulation parameters such as angle of repose, bulk density, compressibility index, and Hausner ratio. Once the desired results were achieved for these parameters and the blend was deemed suitable, it was compressed directly using a twelve-station tablet punching machine equipped with 7 mm punches. After compression, the tablets were meticulously coated and subjected to a detailed assessment of post-compression characteristics to ensure the overall quality and effectiveness of the final product[42–45].

**Table 1: Formulation Table of Core Tablet**

| Sl. No. | Ingredients | Quantity per Tablet (mg) | Percentage (%) Weight |
|---|---|---|---|
| 1 | Carvedilol & β-Cyclodextrin Complex | *25* | *18.52* |
| 2 | Sodium starch glycolate | *10* | *7.41* |
| 3 | Microcrystalline cellulose (MCC) | *35* | *25.93* |
| 4 | Mannitol | *50* | *37.04* |
| 5 | Magnesium stearate | *6.5* | *4.81* |
| 6 | Talc | *8.5* | *6.3* |
| Total Weight | | **135** | **100** |

**Press-Coating process of core tablet:**

The core tablets were enveloped with a barrier and outer layer formulation to achieve a site-specific or time-controlled drug release profile [46]. A compression coating technique was employed to encapsulate the core tablets, utilizing HPMC K100 M (*hydrophilic polymer*), Ethyl cellulose (*hydrophobic polymer*), and Chitosan (natural gel-forming agent). The coating excipients were accurately weighed and passed through a #24 sieve to ensure particle uniformity, followed by blending for 15 minutes to achieve a homogeneous mixture. To perform the coating, half of the blend was introduced into the die cavity of a 12-station tablet compression machine equipped with 11 mm punches. The carvedilol core tablet was then manually positioned at the centre, and the remaining coating material was added to ensure complete coverage. The assembly was subsequently compressed under controlled conditions to produce a well-encapsulated tablet with consistent coating thickness and quality [47,48].

**Post-compression parameters**

Post-compression evaluation constitutes the central quality-control phase that links the physicochemical properties of the finished press-coated tablets to their intended in-vivo performance, and for any chronotherapeutic pharmaceutical formulation—including the time-dependent pulsatile press-coated carvedilol tablets developed in the present investigation—the critical quality attributes must be evaluated by means of standardized pharmacopeial and non-pharmacopeial tests to satisfy regulatory expectations and to verify that the dosage form is fit for its pulsatile-release purpose [37]. Pharmacopoeial compendia such as the United States Pharmacopeia, the Indian Pharmacopoeia, and the British Pharmacopoeia collectively define the official test procedures, apparatus specifications, sample sizes, and acceptance limits for tablet friability, hardness, weight variation, content uniformity, disintegration, and dissolution, and adherence to these compendial procedures was accordingly treated as a methodological prerequisite throughout the present study [49]. For a pulsatile press-coated tablet in particular, each of these post-compression parameters behaves as a fingerprint of the lag-time integrity of the system, because the press-coat is responsible for resisting water ingress and triggering a sigmoidal release profile [17]; consequently, the post-compression tests were conceived not as passive QC markers but as prospective discriminators of the chronotherapeutic performance of the formulation.

**Thickness**

The thickness of tablets was measured using a Vernier caliper. Ten tablets from each batch were selected randomly, and the average thickness along with the standard deviation was calculated to assess uniformity among tablets.Tablet thickness is one of the most basic yet pharmacopeially relevant physical descriptors of a compressed dosage form. Vernier-caliper-based thickness measurement is the standard compendial route documented in the IP, BP, and USP, and is preferred over simple rule-based measurement because it allows direct registration of the caliper jaws across the tablet's diametrical plane with sub-millimetre resolution, which is the configuration specifically recommended in the published tablet-evaluation literature for both flat-faced and biconvex round tablets [50][45]. The use of a digital or manual Vernier caliper enables the rapid non-destructive determination of thickness (and, when the caliper is closed across the die, of diameter) without perturbing the tablet, and is therefore particularly suitable for press-coated systems in which the same physical units must be characterized both before and after the second compression event [51]. For the present formulation, ten randomly selected tablets per batch were measured to generate a representative mean ± SD, exactly as specified in the IP procedure for tablet-thickness appraisal [45].

In the context of the pulsatile press-coated carvedilol tablet, thickness is far more than a geometric descriptor. The lag time that defines the chronotherapeutic performance of the system is highly sensitive to the thickness (*and uniformity*) of the outer coating layer, because the lag is governed by the time required for dissolution medium to penetrate the hydrophobic shell and trigger swelling/rupture; any inter-tablet variability in shell thickness translates directly into a corresponding variability in the onset of drug release [23]. For the core tablets, a thickness of 3–3.5 mm (*with a fixed 7 mm punch diameter*) ensures a geometrically reproducible substrate on which the press-coating can be deposited; for the coated tablets, the thicknesses of F1–F9 fell in the narrow range of 7.03–7.7 mm with a reproducibly low SD *(≤ ±0.17 mm in every batch*), indicating that the press-coating operation produced a remarkably uniform shell across all nine formulations [44]. This consistency is essential not only for the

cosmetic and packaging uniformity demanded by pharmacopeial expectations but, more importantly, for the reproducible pulsatile lag that the formulation is designed to deliver.

**Weight Uniformity**

Twenty tablets were randomly selected from each batch and weighed individually using an analytical balance. The average weight and percentage deviation from the mean were calculated to evaluate weight uniformity in accordance with pharmacopeial standards. The 20-tablet individual-weighing protocol followed here is the canonical compendial procedure for the weight-variation test of uncoated and film-coated tablets in the IP, BP, and USP, and is also the carvedilol-specific protocol adopted in published standardization studies of carvedilol solid dosage forms [52][48][49]. The pharmacopeial acceptance criterion is satisfied when not more than two of the twenty tablets deviate from the average weight by more than the percentage listed in the IP/BP tolerance table—10% for tablets averaging ≤80 mg, 7.5% for tablets >80 mg and <250 mg, and 5% for tablets ≥250 mg—and when no individual tablet deviates by more than twice the relevant percentage [49][50]. The percentage weight variation is calculated by the standard expression:

$$\textbf{Weight Variation} = \frac{W_I - W_A}{W_A} \times 100$$

where $W_I$ is the individual tablet weight and $W_A$ is the average tablet weight [49]. The use of an electronic analytical balance, which is the standard configuration in pharmacopeial weight-variation testing, provides the four-decimal-place traceability needed to resolve such low percentage deviations reliably [48].For a press-coated pulsatile tablet, weight uniformity is mechanistically connected to the lag time. Because the lag phase in press-coated systems is markedly dependent on the EC/HPMC weight ratio in the outer shell—with semilogarithmic relationships between lag time and shell composition documented in the published literature—any deviation in the mass of coating material deposited around the core translates directly into a deviation in lag time [32]. Furthermore, the press-coating operation used in this work explicitly involved splitting the coating blend into two accurately weighed half-portions placed beneath and above the preformed core in the die cavity, so that strict uniformity of the average tablet weight is the read-out that confirms the equal split of coating material around each core. For the core tablet (130.3 ± 2.95 mg, ≈2.3% deviation), the IP tolerance for a tablet in the 80–250 mg range (7.5%) is comfortably met; for the press-coated tablets F1–F9, which range from 338.33 ± 0.57 mg (F7) to 372.50 ± 1.60 mg (F2), the percentage deviation in every batch is well below the 5% limit applicable to tablets above 250 mg, confirming that the press-coating step did not introduce unacceptable weight variability into any formulation.

**Hardness**

The tablet hardness was determined using a Monsanto hardness tester. The hardness of ten tablets was measured, and the average hardness was recorded in kg/cm² to ensure mechanical strength.The Monsanto-type hardness tester is the canonical diametrical-crushing-strength apparatus used in pharmaceutical tablet testing, applying a horizontal compressive load across the diameter of the tablet until the tablet fractures, and registering the breaking force on a calibrated scale; results are conventionally expressed in kg/cm² (*or in the SI kilopond/cm²*), which is the unit employed throughout the published tablet-evaluation literature and in official compendial references [50][49][45][43]. The use of ten randomly selected tablets per formulation is the standard sample size adopted in published carvedilol hardness studies [43] and in analogous chronotherapeutic core-tablet protocols [48][51]. Pharmacopeial expectations generally indicate that uncoated tablets should possess a crushing strength greater than 4 kg and that 3–5 kg/cm² is the conventional satisfactory range for uncoated tablets, while coated and compression-coated tablets are typically expected to exhibit higher values reflecting the added mechanical contribution of the outer layer [50][49].In the present formulation strategy, hardness is a critical attribute for two reasons. First, the core tablets must possess sufficient mechanical strength to survive the second compression step of the press-coating operation without capping, lamination, or internal fracture—the core tablet's hardness of 4.5 ± 0.075 kg/cm² is comfortably above the standard 3–5 kg/cm² range for uncoated tablets, ensuring that the core remains intact during compression of the surrounding EC/HPMC K100 shell [50][49]. Second, the press-coated tablets must be hard enough to withstand handling, packaging, and transportation without damage, yet not so hard as to prevent the swelling/rupture mechanism in the gut; the recorded hardnesses of 7.03–8.06 kg/cm² across F1–F9 place every batch safely within the high-strength window expected of compression-coated tablets without crossing into the brittle-failure regime [31]. The mechanical robustness of the 7-mm core further accommodates the additional compression force imposed during shell formation, which is a frequently neglected but practically critical prerequisite for press-coated pulsatile tablets in which hydrophobic ethyl cellulose and high-viscosity HPMC K100 must be compacted around a preformed core [31][28].

**Friability Test**

The friability of the tablets was determined using a Roche friabilator. A sample of pre-weighed tablets (usually 20) was rotated at 25 rpm for 4 minutes (100 revolutions). The tablets were then dedusted and reweighed. The percentage friability was calculated as:

$$f = 100 \times (1 - \frac{w_0}{w})$$

where $w_0$ = initial weight of tablet and $W$ = weight of tablet after test.

The Roche friabilator is the universally adopted compendial apparatus for the tablet-friability test, in which a rotating drum subjects the tablets to a combined abrasion-and-shock stress by lifting them through a 6-inch drop at each of 25 revolutions per minute for a total of 100 revolutions (4 minutes) [49][50][48]. The standard pharmacopeial protocol prescribes a sample of either twenty tablets or, for larger tablets, sufficient whole tablets to provide approximately 6.5 g of total mass [49][37]. After the 100-revolution cycle, the tablets are dedusted (typically with a soft muslin cloth) and reweighed, and the percentage weight loss is calculated by the equation above [49][50]. The USP and IP acceptance limits for uncoated tablets are typically ≤1% weight loss, with a tighter 0.5–1% range commonly cited as the working window for compressed tablets [50][49].For the carvedilol pulsatile press-coated tablet, friability is the principal descriptor of mechanical durability under the combined stresses imposed by handling, packaging, transportation, and dispensing. Because the outer shell is responsible for carrying the entire lag-time burden, any chipping, capping, or abrasion of the shell during post-compression handling would directly compromise the integrity of the press-coat and shorten the in-vitro lag time [23]. The friability values recorded for F1–F9 in the present work span 0.64–0.86%, all comfortably below the 1% pharmacopeial limit and consistent with the typical durability of press-coated carvedilol tablets described in published carvedilol-formulation studies [53]. This is a particularly important outcome because the substantial compositional spread across the nine HPMC K100:ethyl cellulose ratios (0:100 to 100:0) might, in principle, have produced lamination-prone batches at the extremes of polymer ratio; the fact that friability remained uniformly below 1% across the entire compositional range confirms that direct compression of a dry EC/HPMC K100 blend around a preformed core can produce a mechanically durable bilayer without compromising shell integrity [48][31].

**Drug Content**

Ten tablets were randomly selected and crushed using a mortar and pestle. A 100 mg sample of the powdered blend was accurately weighed and dissolved in a 6.8 pH phosphate buffer. The mixture was shaken and kept for 24 hours to ensure complete dissolution. The solution was filtered, and suitable dilutions were prepared using the same buffer. The absorbance was measured at a wavelength of 241 nm using a UV-Visible spectrophotometer against a 6.8 pH phosphate buffer as a blank. The average of triplicate readings was taken, and the percentage of drug content was calculated for all batches.

The drug-content (content-uniformity) test is the compendial assay by which the actual amount of active pharmaceutical ingredient present in a finished tablet is verified against the label claim. Per the BP, the dosage form complies with the test if the individual content of each of ten randomly selected tablets lies within the range of 85–115% of the average content and none deviate outside 75–125% of the average content; the IP lays down a parallel procedure in which the totality of active ingredient(s) per tablet is calculated from the assay, and the result must lie within the monograph range [49]. For low-dose or low-drug-fraction tablets where the weight-variation test is not sufficiently discriminating, the content-uniformity test supersedes the weight-variation test, and a content range of 85–115% is the canonical BP acceptance window [49][43]. The procedure described here—powdering ten tablets, dissolving an accurately weighed aliquot of the blend in phosphate buffer pH 6.8, completing dissolution over 24 h, filtering, and quantifying by UV at the validated $\lambda_{max}$ of 241 nm—mirrors the published UV-spectrophotometric content-determination protocols for carvedilol, including validated methods that specifically confirmed no interference from common excipients in the tablet matrix [54][34]. The 24-h dissolution step with continuous agitation ensures that both freely soluble carvedilol and the carvedilol contained within the β-cyclodextrin inclusion complex are fully liberated and quantified; the $\lambda_{max}$ of 241 nm is the same wavelength identified in the analytical-method-development section of the present work (Section 3.1) and is consistent with the published validation spectra for carvedilol in phosphate buffer [54].In the present formulation, drug content serves as a critical confirmatory QC marker for both the core and the press-coated tablets. For the core tablet, the observed ~125% content relative to the labelled 6.25 mg carvedilol dose is internally consistent with the deliberate stoichiometric excess of the carvedilol–β-cyclodextrin complex (*1:3 drug-to-cyclodextrin*) incorporated into the formulation, in which only the carvedilol moiety contributes to the UV absorbance at 241 nm while the cyclodextrin serves as a solubilizing carrier; the surface excess therefore reflects the payload that the inclusion complex is designed to deliver [38][43]. For the press-coated tablets F1–F9, the drug-content test confirms that the press-coating operation (*which involves handling the core tablet through die positioning, manual centering, and re-compression*) does not degrade or lose active ingredient from the core; this is a necessary precondition for the entire pulsatile strategy, because any loss of payload during the second compression step would invalidate the dose-uniformity assumption on which the lag-time-driven chronotherapy is built [49][43].

***In-vitro* Dissolution Study of Core Tablets**

The dissolution study of core tablets was performed using **USP Type II** apparatus in 900 mL of 6.8 pH phosphate buffer for ***2 hours at 37±0.5 °C*** and a paddle rotation speed of 50 rpm. Samples of 10 mL were withdrawn at every 5-minute interval for 1 hour, and an equal volume of pre-warmed fresh buffer was replaced to maintain sink conditions. The withdrawn samples were filtered through Whatman filter paper, and absorbance was measured at 241 nm using a UV–

Visible spectrophotometer. The cumulative percentage drug release was calculated.USP Apparatus II (*the rotating-paddle apparatus)* is the compendial dissolution instrument prescribed for a wide range of solid oral dosage forms, and its pharmacopeial specifications—37 ± 2 °C (*with the present study adopting the tighter ±0.5 °C band*), 50-rpm paddle rotation in 900 mL of dissolution medium—are the standard conditions documented in published carvedilol dissolution methodology and in generic pharmacopoeial monographs for bilayer and matrix tablets [52][49][55][43]. The 37 ± 0.5 °C temperature band applied here is comfortably within the USP-mandated 37 ± 2 °C range for plain and coated tablets [49], and the 50-rpm paddle speed is the rotating-paddle condition used in the carvedilol-specific dissolution protocols documented for both immediate-release and modified-release carvedilol dosage forms [52][55][43]. The 10-mL sample volume, replaced with an equal volume of pre-warmed fresh buffer at each withdrawal point, maintains sink conditions throughout the run [55][43]; Whatman filter-paper filtration followed by UV detection at the validated $\lambda_{max}$ of 241 nm is the standard analytical close of carvedilol dissolution runs in the published literature [33][55]. The 5-min sampling interval for the first hour enables dense kinetic profiling of the early drug-release window, which is critical for resolving the disintegration-driven burst characteristic of ***fast-dissolving core tablets*** containing ***superdisintegrants such as sodium starch glycolate***[43].

Within the broader chronotherapeutic design of this investigation, the *in-vitro* dissolution study of the core tablets is not a stand-alone QC test but a foundational release-verification step. It establishes the release-readiness of the inner matrix, so that any retardation observed in the subsequently press-coated batchescan be unambiguously attributed to the outer shell rather than to any release-deficit in the core [30]. In pulsatile drug delivery systems designed to align drug input with circadian rhythms, the absence of a continuous drug leak from the core during the lag phase is essential to the chronotherapeutic intent—rapid release is required after the predetermined lag, but premature release during sleep would defeat the chronobiologic strategy of suppressing the morning blood-pressure surge [19][24][21]. The complete release of the core tablet in pH 6.8 phosphate buffer confirmed in this study therefore provides the baseline against which the lag-time and burst-release behaviour of the nine EC/HPMC K100-coated formulations (F1–F9) can be interpreted.

***In-vitro* Dissolution Study of Press-Coated Tablets**

The dissolution study of coated tablets was conducted using 0.1 N HCl and 6.8 pH phosphate buffer solution. The test was first carried out in 0.1 N HCl for 2 hours to simulate gastric transit, followed by 6.8 pH phosphate buffer for 6 hours to mimic intestinal conditions. The dissolution medium volume was 900 mL, maintained at 37±0.5°C with a paddle speed of 50 rpm. At hourly intervals, 10 mL of dissolution medium was withdrawn and replaced with an equal volume of fresh solution. Samples were filtered, and absorbance was measured at 241 nm using a UV–Visible spectrophotometer. The percentage drug release and lag time were determined for all coated tablet formulations.

**Kinetics Study**

In the model-dependent process, a mathematical model with known release kinetics was used to compare dissolution patterns. Several mathematical functions served as the foundation for model-dependent techniques that were used to compare and describe the disintegration patterns of tablets. To compare dissolution profiles, dissolution data were analyzed, and DD-Solver software was used to choose fitted models based on the coefficient of determination ($\mathbf{R^2}$), **Akaike Information Criterion** (AIC), and **Root Mean Square Error** (RMSE) values. Various types of kinetics studies are commonly observed in the field of pharmaceutical research. These include zero-order kinetics, first-order kinetics, as well as more complex models such as the Higuchi model and the Korsmeyer-Peppas model. Each of these models plays a crucial role in understanding drug release mechanisms and formulating effective drug delivery systems.

**Zero-order model**

This equation may be used to depict medication dissolution from dosage forms that do not disintegrate and release the drug gradually. $\mathbf{Q_0 - Q_t = K_0 t}$. The zero-order release constant is $K_0$, the starting quantity of medication in solution (often zero) is $Q_0$, and Q is the amount of drug released or dissolved. Cumulative drug release against time was plotted.

**First-order model**

The absorption and/or elimination of some medications have also been described using the first-order model, even though it is challenging to theoretically grasp this mechanism. Using first-order kinetics, the drug's release may be described by the following equation **Dc/DT = -Kc**. The first-order rate constant, K, is expressed in time-1 units. This is log C = log C0 - Kt / 2.303. The starting drug concentration is denoted by C0, the first-order rate constant by k, and the time by t. **A time vs. log cumulative percentage of medication remaining was created.**

**Higuchi Model**

Higuchi created the first mathematical model in 1963 that attempted to explain drug release from a matrix system. This model may be used to investigate the release of both water-soluble and low-soluble pharmaceuticals that are integrated into semisolid and solid matrices. The equation gives the model expression $\mathbf{Q = A.\ [D\ Cs\ t\ (2C - Cs)]^{½}}$. Where Q is the quantity of medication given out per unit area in time t. A, C, and D stand for the drug's starting concentration, solubility in the media, and diffusivity of the drug molecules (also

known as the diffusion coefficient) in the matrix, respectively.

**Korsmeyer-Peppas Model**

Drug release from a polymeric system was explained by a straightforward relationship that Korsmeyer developed. Ritger, Peppas, Korsmeyer, and Peppas created an empirical formula to examine drug release from swelling and nonswelling polymeric delivery methods, both Fickian and non-Fickian. The Korsmeyer-Peppas model was fitted to the first 60% of drug release data to determine the mechanism of drug release. $\mathbf{K\ t^n = M_t / M_\alpha}$, where k is the rate constant (with units of tn) that takes into account the geometrical and structural features of the delivery system, and Mt/Mα is the proportion of medication released at time t.

**Hixson and Crowell model**

The Hixson-Crowell model is correct and well aligned with established pharmaceutical kinetics literature. The model specifically addresses drug release from dosage forms where there is a change in both surface area and particle diameter as dissolution progresses, such as tablets that erode or shrink during drug release. Hixson and Crowell recognized that for such systems, the surface area is proportional to the cube root of the volume (or mass) of the drug particle. The model is mathematically expressed as: $\mathbf{W_0^{1/3} - W_t^{1/3} = Kt}$, Where, $\mathbf{W_0}$ is the initial amount of drug in the dosage form, $\mathbf{W_t}$ is the amount remaining at time, and Kt (or $K_{HC}$) is a rate constant that incorporates the relationship between surface area and volume, as well as other dissolution factors. This cube root law is particularly used for dosage forms such as conventional, immediate, or dispersible tablets, where surface area reduction—rather than just simple diffusion—controls the dissolution rate.

**Statistical analysis**

Statistical analysis in the present investigation was performed using **SPSS**, with one-way analysis of variance applied to the *in-vitro* release data obtained for all nine press-coated tablet batches (F1 to F9) of the chronotherapeutic carvedilol formulation. The ***ANOVA*** was used to compare the means of the nine patch formulations on cumulative percentage drug release across the 8-hour dissolution window, thereby detecting any significant inter-formulation differences in release behaviour. Where the omnibus F-test returned a significant result, **Tukey's Honestly Significant Difference** test (***Tukey-HSD / Tukey's test***) was subsequently applied as the post-hoc step to pinpoint the **specific pairwise differences** between the **F1–F9 press-coated tablet batches** that contributed to the overall significance. The combined ***ANOVA + Tukey-HSD framework*** was used to evaluate (i) cumulative percentage drug release over 8 hours for all nine formulations (the mean ± SD bars in Table 6 and the SPSS-generated dissolution-profile comparison in Fig. 8); (ii) the formulation physicochemical parameters — weight uniformity, thickness, hardness, and friability — across F1–F9, expressed as mean ± SD in Table 6; and (iii) the lag-time milestones at t-10%, t-50%, and t-80% release (Tables 8 and 9), with the Tukey-HSD analyses of the individual release-time pulses (*Section 3.4.7*) supplying the letter-overlay notation (*a, b, c, d, e, f, g, h, i*) used in Table 6 and Fig. 8 to identify which pairs of formulations differed at $\boldsymbol{P < 0.05}$. The outcome of the ANOVA + Tukey's test combination was decisive for the present study: it objectively separated the F1–F9 formulation space into the three behavioural clusters observed in the dissolution and lag-time data — short-lag (F1, F6, F7), mid-range (F2, F3, F4, F8) and long-lag (F5 and F9) — and singled out F2, F5, and F9 as the behavioural candidates whose release profiles differed most significantly from the remaining batches within each release window. ANOVA-based model fitting of the cumulative friability—across and physicochemical responses across all nine formulations further substantiated the ranking of these candidates, and the consistent convergence of the statistical, physicochemical, kinetic, and lag-time evidence on F5 (***HPMC K100:ethyl cellulose = 33.33:66.66***) confirmed F5 as the optimal pulsatile press-coated carvedilol batch. **Throughout, P values < 0.05 were deemed statistically significant**.

**RESULTS**

**Estimation of Carvedilol in 0.1 (N) HCL**

The determination of the $\lambda_{max}$ value of Carvedilol involved the careful scanning of solutions prepared at concentrations of 4 µg/ml and 10 µg/ml. This scanning process was meticulously conducted using a UV-Visible spectrophotometer, with measurements taken within the wavelength range of 200-400 nm. To ensure accuracy, the readings were compared against the blank of each respective solution. Upon thorough analysis, the $\lambda_{max}$ value for Carvedilol was pinpointed at 241 nm specifically in a 0.1 N HCl solution. It was observed that Carvedilol adhered to Beer's law within a concentration range of 4-36 µg/ml. This indicated that the drug's absorbance at various concentrations followed a linear relationship, facilitating precise quantitative measurements within the specified range. Overall, the process of determining Carvedilol's $\lambda_{max}$ involved rigorous experimentation and analysis, yielding crucial insights into the drug's behaviour within different solutions and concentrations. This information can prove instrumental in further research and applications related to Carvedilol's pharmaceutical properties.

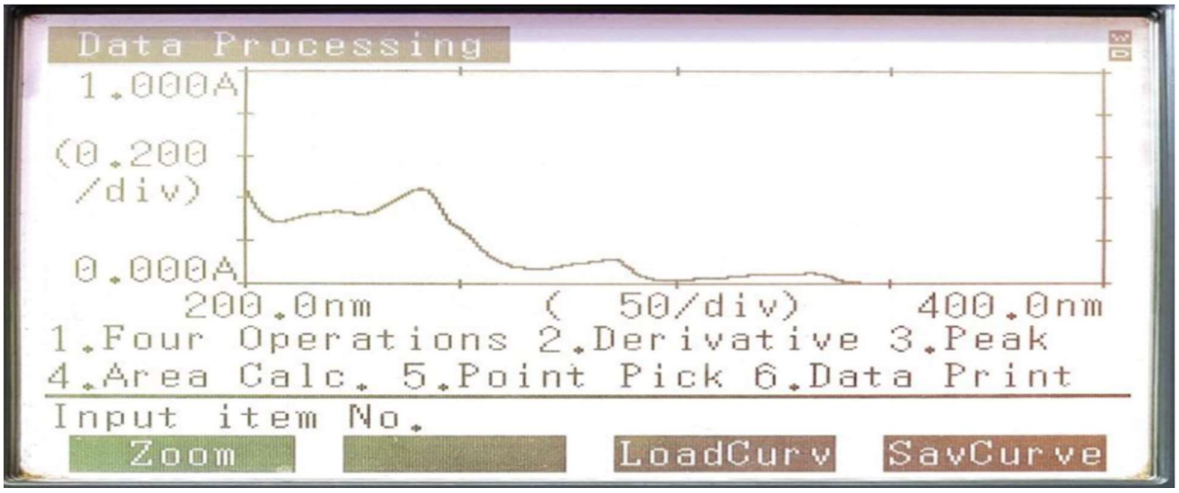


**Fig. 1: Spectrum of carvedilol in 0.1 (N) HCl through UV-Visible spectrophotometer**

**Table 2: Data for Standard calibration curve of Carvedilol in 0.1 (N) HCl**

| Sl. No. | Concentration (µg/ml) | Absorbance ($\lambda_{max}$ = 241nm) | Mean Absorbance ($\lambda_{max}$ = 241nm) | SD (n = 3) |
|---|---|---|---|---|
| 1 | 2 | 0.072 | 0.071 | 0.001 |
| | | 0.071 | | |
| | | 0.071 | | |
| 2 | 4 | 0.127 | 0.127 | 0.001 |
| | | 0.128 | | |
| | | 0.127 | | |
| 3 | 6 | 0.182 | 0.182 | 0.001 |
| | | 0.181 | | |
| | | 0.183 | | |
| 4 | 8 | 0.24 | 0.241 | 0.002 |
| | | 0.241 | | |
| | | 0.243 | | |
| 5 | 10 | 0.293 | 0.294 | 0.001 |
| | | 0.295 | | |
| | | 0.294 | | |

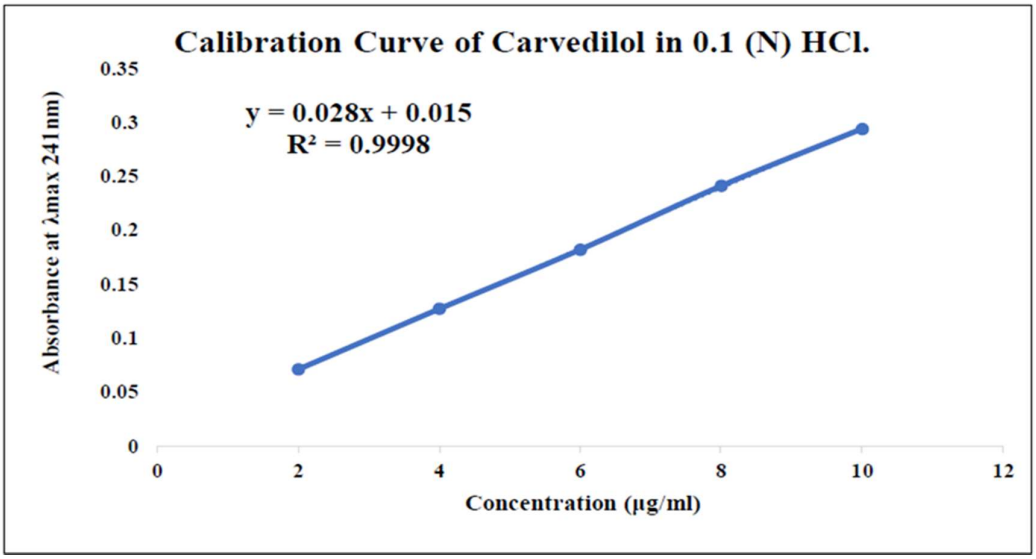


**Fig. 2: Standard calibration curve of Carvedilol in 0.1 (N) HCL**

**Estimation of Carvedilol in 6.8 pH Phosphate buffer**

The $\lambda_{max}$ of Carvedilol was successfully determined through a meticulous scanning process involving solutions with concentrations of 10 µg/ml and 35 µg/ml. This procedure was carried out using a state-of-the-art UV-Visible spectrophotometer that covered the wavelength range of 200-400 nm, with readings compared against the corresponding solution's blank. Remarkably, the drug's $\lambda_{max}$ was observed at 241 nm in a pH 6.8 buffer, indicating a critical aspect of its spectral behaviour. Furthermore, it was observed that Carvedilol exhibited a pronounced adherence to Beer's law within the analytically significant concentration range of 4-36 µg/ml, affirming the validity and reliability of the obtained results in a context that underscores the pharmaceutical significance of this study.

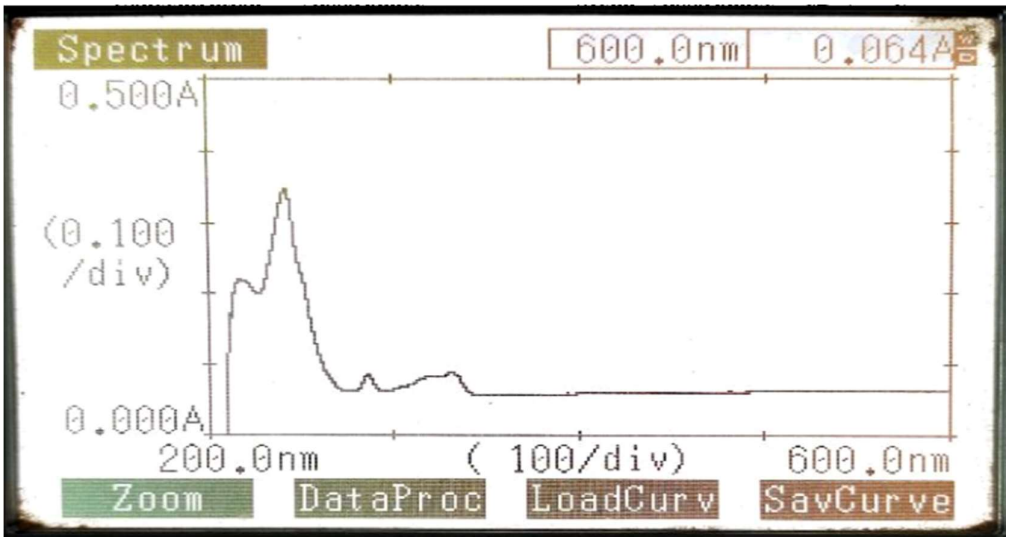


**Fig. 3: Spectrum of carvedilol in 6.8 pH Phosphate buffer through UV-Visible spectrophotometer**

**Table 3: Data for Standard calibration curve of Carvedilol in 6.8 pH Phosphate Buffer**

| Sl. No. | Concentration (µg/ml) | Absorbance ($\lambda_{max}$ = 241nm) | Mean Absorbance ($\lambda_{max}$ = 241nm) | SD (n = 3) |
|---|---|---|---|---|
| 1 | 10 | 0.146 | 0.146 | 0.001 |
| | | 0.145 | | |
| | | 0.147 | | |
| 2 | 15 | 0.191 | 0.192 | 0.002 |
| | | 0.192 | | |
| | | 0.194 | | |
| s3 | 20 | 0.261 | 0.261 | 0.001 |
| | | 0.262 | | |
| | | 0.261 | | |
| 4 | 25 | 0.324 | 0.324 | 0.001 |
| | | 0.323 | | |
| | | 0.325 | | |
| 5 | 30 | 0.362 | 0.363 | 0.001 |
| | | 0.364 | | |
| | | 0.363 | | |
| 6 | 35 | 0.447 | 0.447 | 0.001 |
| | | 0.448 | | |
| | | 0.447 | | |

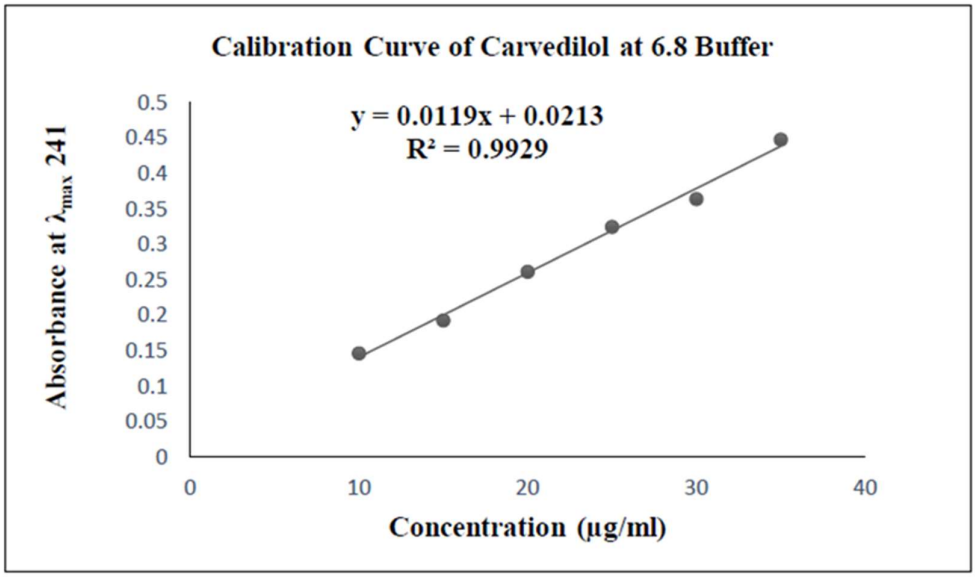


**Fig. 4: Standard calibration curve of Carvedilol in 6.8 pH Phosphate Buffer**

**Preformulation study (*Identification of drug*):**

**Melting point Determination**

The capillary tube method, a reliable technique in scientific analysis, was meticulously employed to determine the melting point of carvedilol, yielding 112 degrees Celsius. Notably, this experimental result aligns with established data in the literature, confirming a melting point of 114 degrees Celsius for carvedilol and indicating the robustness and consistency of the analytical methods employed, thereby reinforcing the validity and reproducibility of the findings in this experimental study.

**ATR-FTIR Spectroscopy**

The ATR-FTIR spectrophotometer, a sophisticated analytical instrument, was specifically utilized to perform detailed analysis on the functional groups linked with Carvedilol, an important active pharmaceutical ingredient (API). Through this precise analysis, Carvedilol's distinct absorption peaks were meticulously identified at various key wavenumbers. Notably, the observed peaks in the spectroscopic data of the pure Carvedilol sample were found to be in perfect agreement with the characteristic peaks outlined in the official Indian Pharmacopoeia spectrum, thereby affirming the high purity and quality of the medicinal compound under evaluation**.**

Further delving into the specific peaks detected for Carvedilol in the IR spectra, the results indicated notable absorption bands at significant wavenumbers. These included the prominent peak at 3329.76 $cm^{-1}$ associated with the N-H stretching vibration band, the distinctive signal at 2922.16 $cm^{-1}$ representing C-H bonds, the discernible peak at 1095.50 $cm^{-1}$ indicative of the C-O bending vibration band, the distinct occurrence at 1502.55 $cm^{-1}$ attributing to the C=C stretching vibration band, and the clearly defined peak at 1212.56 $cm^{-1}$ signalling the C-N stretching vibration band. Additionally, the IR analysis brought to light another set of distinct peaks at specific wavenumbers, including key points at 1092.50 $cm^{-1}$ (C-O bending), 1539.69 cm-1 (C=C stretching), and 1216.27 cm-1 (C-N stretching), thus contributing further valuable insights into the structural composition and characteristics of Carvedilol.

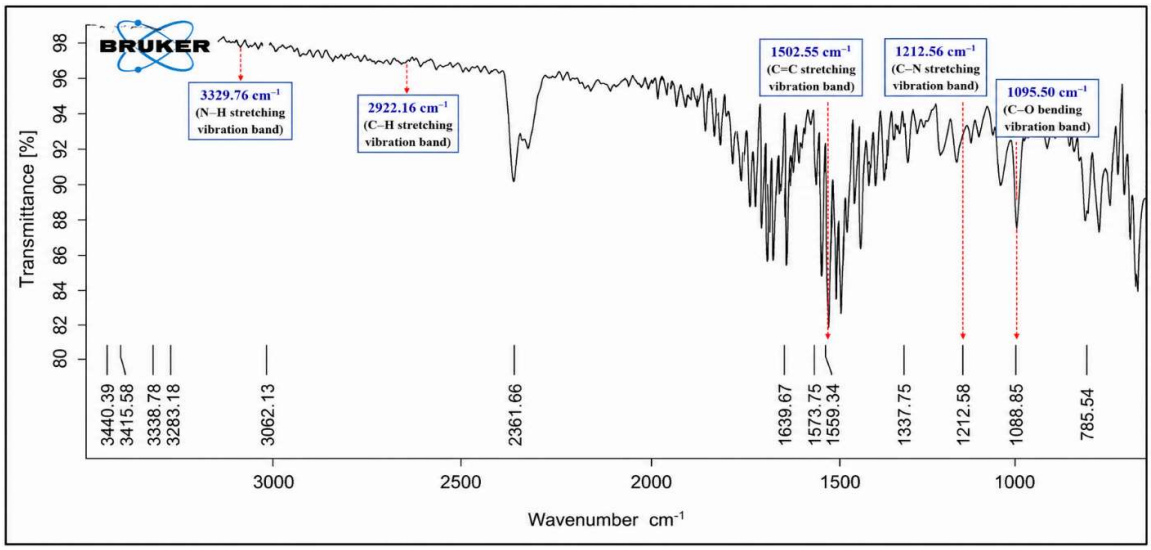


**Fig. 5: ATR-FTIR spectra of Carvedilol**

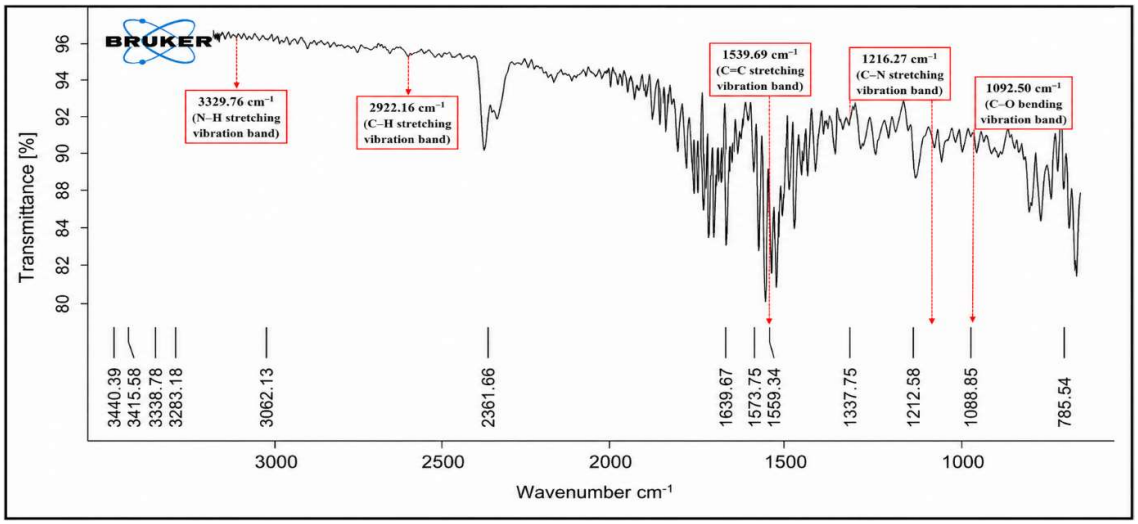


**Fig. 6: ATR-FTIR spectra of Carvedilol & Excipients Blend for Compatibility Study**

**Micromeritic properties** [46,56]

**Table 4: Micromeritic Properties of the Carvedilol Drug and the powder blend of the formulation**

| Parameters | Carvedilol (Drug) | Powder blend | Status |
|---|---|---|---|
| Angle of repose | 31.42 | 32.14 | Good |
| Carr's index % | 14.82 | 13.84 | Good |
| Hausner's ratio | 1.14 | 1.16 | Good |

**Post-compression parameters of the core tablet**

Post-compression parameters like hardness, weight uniformity, friability, thickness, and drug content were evaluated for core tablets and design batches (*bilayer or matrix tablets*), respectively.

**Physicochemical characterization of Core tablets**

**Table 5: Post-compression parameters for designed coated tablets**

| Formula | Weight variation | Thickness | Hardness | Friability | Disintegration Time (Sec) | Drug content |
|---|---|---|---|---|---|---|
| | | (mm) | (Kg/cm2) | (%) | | (%) |
| Core | 130.3±2.95 | 3-3.5 | 4.5±0.075 | 0.45 | 210±2 | 125 |

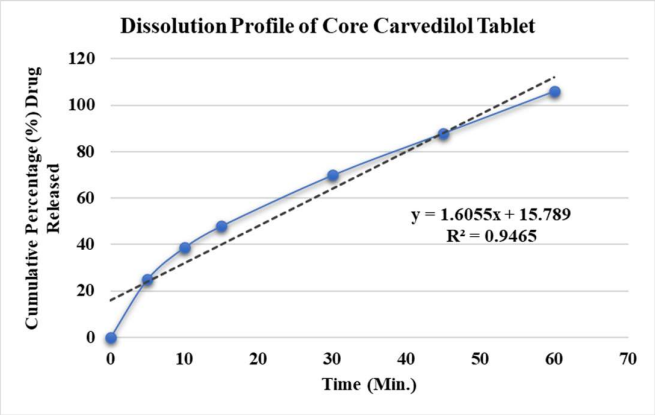


**Fig. 7: In vitro dissolution of the core carvedilol tablet in PBS, pH 6.8**

**Analysis of Physicochemical Properties of the batches and their statistical interpretation through Tukey HSD:**

**Table 6: Physicochemical characterization of press-coated tablets (*Matrix of Polymers*)**

| Formula | Weight uniformity | Thickness (mm) | Hardness (Kg/cm$^2$) | Friability (%) | Cumulative% Drug release within 8 hours |
|---|---|---|---|---|---|
| F1 | 370.32±1.35 | 7.1±0.10 $^{b,d,f}$ | 7.6±0.10 $^{b,c,d,e,i}$ | 0.74±0.026 | 85.31±3.73 |
| F2 | 372.50±1.60 | 7.53±0.06$^{a, c,e, g,h,i}$ | 8.06±0.12 $^{a,c,d,e,f,g,h}$ | 0.86±0.010 | 94.94±1.34 |
| F3 | 345.63±0.56 | 7.03±0.06 $^{b,d,f}$ | 7.3±0.10 $^{a,d,e,f,h,i}$ | 0.79±0.010 | 98.14±1.74 |
| F4 | 371.43±0.32 | 7.7±0.10$^{a, c,e,g,h,i}$ | 7.03±0.06 $^{a,b,c,f,g,h,i}$ | 0.69±0.010 | 98.09±1.28 |
| F5 | 355.33±0.57 | 7.1±0.10 $^{b,d,f}$ | 7.03±0.06 $^{a, b,c,f,g,h,i}$ | 0.75±0.010 | 96.15±0.70 |
| F6 | 366.00 ±1.00 | 7.63±0.06$^{a, c,e,g,h,i}$ | 7.6±0.10 $^{b, c,d,e,i}$ | 0.64±0.015 | 89.55±3.75 |
| F7 | 338.33±0.57 | 7.23±0.06 $^{b,d,f}$ | 7.43±0.06 $^{b,d,e,i}$ | 0.77±0.010 | 92.72±1.86 |
| F8 | 366.00 ±1.00 | 7.3±0.10 $^{d,f}$ | 7.6±0.10 $^{b,c,d,e,i}$ | 0.67±0.021 | 97.48±1.06 |
| F9 | 346.33±1.52 | 7.1±0.17 $^{b,d,f}$ | 8.03±0.06 $^{a,c,d,e,f,g,h}$ | 0.66±0.025 | 74.22±7.16 |
| *Note: All the observations are mean ± SD (n=3). Here, if P<0.05 vs F1 = a; P<0.05 vs F2 = b; P<0.05 vs F3 = c; P<0.05 vs F4 = d; P<0.05 vs F5 = e; P<0.05 vs F6 = f; P<0.05 vs F7 = g if P<0.05 vs F8 = h; P<0.05 vs F9 = i* | | | | | |

**Dissolution Profile Comparison graph of all batches (F1 to F9) generated through SPSS Analysis**

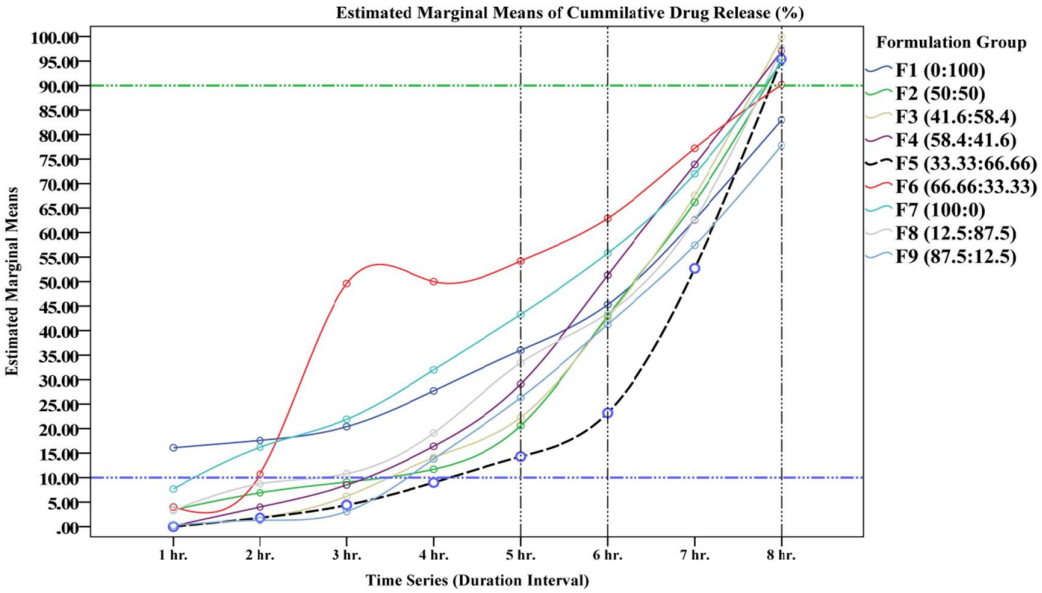


**Fig. 8: Cumulative % Drug release (mean ± SD; n=3) of estimated marginal means of each formulation corresponding to the time series**

**Release kinetics Study of all formulations to ensure the best-fit model of all batches from F1 to F9**

**Table 7: Zero-order, First-order, Higuchi, Korsmeyer-Peppas release kinetics for F1 to F9**

| | Parameter | F1 | F2 | F3 | F4 | F5 | F6 | F7 | F8 | F9 |
|---|---|---|---|---|---|---|---|---|---|---|
| ZERO ORDER | **R_sqr_adj** | **0.92** | **0.7466** | **0.7342** | **0.7986** | **0.6144** | **0.9413** | **0.9446** | **0.815** | **0.7937** |
| | **$k_0$** | 8.712 | 8.23 | 8.417 | 9.053 | 6.834 | 11.196 | 10.032 | 8.715 | 7.21 |
| | **AIC** | 56.4912 | 71.3093 | 72.8696 | 70.4647 | 74.581 | 57.816 | 56.6793 | 68.1122 | 66.8253 |
| | **MSC** | 2.0535 | 1.053 | 1.0185 | 1.2782 | 0.6022 | 2.3463 | 2.4658 | 1.3433 | 1.2586 |
| FIRST ORDER | **Parameter** | **F1** | **F2** | **F3** | **F4** | **F5** | **F6** | **F7** | **F8** | **F9** |
| | **$k_1$** | 0.118 | 0.102 | 0.104 | 0.116 | 0.08 | 0.178 | 0.142 | 0.112 | 0.088 |
| | **R_sqr_adj** | **0.8403** | **0.6425** | **0.6272** | **0.6832** | **0.5345** | **0.8979** | **0.8396** | **0.7074** | **0.7075** |
| | **AIC** | 62.7065 | 74.4065 | 75.9134 | 74.5436 | 76.2768 | 62.7898 | 66.2444 | 72.2401 | 69.9671 |
| | **MSC** | 1.3629 | 0.7088 | 0.6803 | 0.825 | 0.4137 | 1.7936 | 1.403 | 0.8847 | 0.9095 |
| HIGUCHI | **Parameter** | **F1** | **F2** | **F3** | **F4** | **F5** | **F6** | **F7** | **F8** | **F9** |
| | **$k_H$** | 20.097 | 18.021 | 18.244 | 19.839 | 14.622 | 26.096 | 22.896 | 19.334 | 15.748 |
| | **R_sqr_adj** | **0.7429** | **0.503** | **0.4843** | **0.5436** | **0.3895** | **0.8155** | **0.7335** | **0.5718** | **0.5361** |
| | **AIC** | 66.9948 | 77.3722 | 78.8342 | 77.8286 | 78.7175 | 68.1145 | 70.8171 | 75.6677 | 74.1172 |
| | **MSC** | 0.8864 | 0.3793 | 0.3558 | 0.46 | 0.1426 | 1.202 | 0.8949 | 0.5038 | 0.4484 |
| KROSMEYER PEPPAS | **Parameter** | **F1** | **F2** | **F3** | **F4** | **F5** | **F6** | **F7** | **F8** | **F9** |
| | **kKP** | 4.332 | 0.214 | 0.198 | 0.565 | 0.011 | 11.302 | 4.092 | 0.672 | 0.492 |
| | **n** | 1.382 | 2.932 | 3.003 | 2.483 | 4.371 | 0.995 | 1.49 | 2.373 | 2.442 |
| | **R_sqr_adj** | **0.9401** | **0.9898** | **0.9992** | **0.9971** | **0.9929** | **0.9329** | **0.9895** | **0.9855** | **0.9952** |
| | **AIC** | 54.6814 | 43.0788 | 21.308 | 32.8943 | 39.3795 | 59.8147 | 42.4969 | 45.9928 | 33.7169 |
| | **MSC** | 2.2545 | 4.179 | 6.701 | 5.337 | 4.5134 | 2.1242 | 4.0416 | 3.801 | 4.9373 |

**Statistical Mean Plot analysis of F1 to F9 formulation batches corresponding to their post-formulation characteristics, e.g., weight uniformity, thickness, hardness & friability (SPSS):**

**Statistical Mean Plot analysis of F1 to F9 formulation batches corresponding to their lag time duration and cumulative percentage drug release of all formulation batches (F1 to F9):**

**Analysis of the cumulative percentage release at 10%, 50%, & 80% of carvedilol, corresponding to the time considered the lag time.**

**Table 8: Lag time Analysis of each of the batches (F1 to F9) corresponding to their cumulative percentages, i.e., 10%, 50%, & 80% release of drug**

| Formulation Code | Lag Time (Hr.) $t_{10}$ % | $t_{50}$ % | $t_{80}$ % | Line Equation | Formulation Code | Lag Time (Hr.) $t_{10}$ % | $t_{50}$ % | $t_{80}$ % | Line Equation | Formulation Code | Lag Time (Hr.) $t_{10}$ % | $t_{50}$ % | $t_{80}$ % | Line Equation |
|---|---|---|---|---|---|---|---|---|---|---|---|---|---|---|
| F1 | 1.31 | 5.74 | 9.05 | y = 9.0434x - 1.8782 | F2 | 2.30 | 5.98 | 8.73 | y = 10.889x - 15.071 | F3 | 2.43 | 5.86 | 8.44 | y = 11.658x - 18.363 |
| F1 | 1.38 | 5.46 | 8.53 | y = 9.7966x - 3.5229 | F2 | 2.27 | 5.97 | 8.75 | y = 10.808x - 14.551 | F3 | 2.41 | 5.89 | 8.50 | y = 11.489x - 17.707 |
| F1 | 1.37 | 5.70 | 8.95 | y = 9.2442x - 2.7045 | F2 | 2.31 | 5.92 | 8.63 | y = 11.076x - 15.575 | F3 | 2.45 | 5.94 | 8.56 | y = 11.451x - 18.036 |
| Mean | 1.36 | 5.63 | 8.84 | HPMC-K100: EC F1 = (0: 100) | Mean | 2.29 | 5.96 | 8.70 | HPMC-K100: EC F2 = (120: 120) | Mean | 2.43 | 5.90 | 8.50 | HPMC-K100: EC F3 = (41.6:58.4) |
| SD | 0.037 | 0.149 | 0.279 | | SD | 0.020 | 0.031 | 0.064 | | SD | 0.018 | 0.039 | 0.062 | |

| Formulation Code | Lag Time (Hr.) $t_{10}$ % | $t_{50}$ % | $t_{80}$ % | Line Equation | Formulation Code | Lag Time (Hr.) $t_{10}$ % | $t_{50}$ % | $t_{80}$ % | Line Equation | Formulation Code | Lag Time (Hr.) $t_{10}$ % | $t_{50}$ % | $t_{80}$ % | Line Equation |
|---|---|---|---|---|---|---|---|---|---|---|---|---|---|---|
| F4 | 2.25 | 5.56 | 8.04 | y = 12.086x - 17.186 | F5 | 2.75 | 6.80 | 9.84 | y = 9.873x - 17.185 | F6 | 1.01 | 4.50 | 7.11 | y = 11.486x - 1.6439 |
| F4 | 1.36 | 4.60 | 7.03 | y = 12.351x - 6.8271 | F5 | 2.70 | 6.65 | 9.61 | y = 10.124x - 17.335 | F6 | 1.09 | 4.50 | 7.06 | y = 11.73x - 2.829 |
| F4 | 2.21 | 5.53 | 8.02 | y = 12.035x - 16.56 | F5 | 2.64 | 6.52 | 9.43 | y = 10.308x - 17.253 | F6 | 1.13 | 4.85 | 7.65 | y = 10.732x - 2.0762 |
| Mean | 1.94 | 5.23 | 7.70 | HPMC-K100: EC F4 = (58.4:41.6) | Mean | 2.70 | 6.66 | 9.63 | HPMC-K100: EC F5 = (33.33:66.66) | Mean | 1.08 | 4.62 | 7.27 | HPMC-K100: EC F6 = (66.66: 33.33) |
| SD | 0.500 | 0.545 | 0.579 | | SD | 0.055 | 0.141 | 0.205 | | SD | 0.057 | 0.204 | 0.326 | |

| Formulation Code | Lag Time (Hr.) $t_{10}$ % | $t_{50}$ % | $t_{80}$ % | Line Equation | Formulation Code | Lag Time (Hr.) $t_{10}$ % | $t_{50}$ % | $t_{80}$ % | Line Equation | Formulation Code | Lag Time (Hr.) $t_{10}$ % | $t_{50}$ % | $t_{80}$ % | Line Equation |
|---|---|---|---|---|---|---|---|---|---|---|---|---|---|---|
| F7 | 1.49 | 5.06 | 7.73 | y = 11.207x - 6.6568 | F8 | 2.09 | 5.72 | 8.45 | y = 11.014x - 13.024 | F9 | 2.51 | 6.60 | 9.68 | y = 9.7651x - 14.479 |
| F7 | 1.51 | 5.16 | 7.89 | y = 10.982x - 6.6261 | F8 | 2.08 | 5.67 | 8.36 | y = 11.139x - 13.127 | F9 | 2.47 | 6.49 | 9.50 | y = 9.9693x - 14.663 |
| F7 | 1.45 | 5.14 | 7.91 | y = 10.846x - 5.7799 | F8 | 2.16 | 5.86 | 8.64 | y = 10.791x - 13.256 | F9 | 2.65 | 7.59 | 11.29 | y = 8.1014x - 11.475 |
| Mean | 1.49 | 5.12 | 7.84 | HPMC-K100: EC F7 = (100: 0.0) | Mean | 2.11 | 5.75 | 8.48 | HPMC-K100: EC F8 = (12.5: 87.5) | Mean | 2.54 | 6.89 | 10.15 | HPMC-K100: EC F9 = (87.5: 12.5) |
| SD | 0.030 | 0.055 | 0.096 | | SD | 0.042 | 0.100 | 0.144 | | SD | 0.094 | 0.605 | 0.989 | |
| ***Note: - All the observation are Mean ± SD(n=3)*** | | | | | | | | | | | | | | |

**Tukey-HSD analysis of each time (hour) related to different amounts of release, i.e., 10%, 50%, and 80% cumulative amounts of carvedilol released from each formulation:**

**Lag-Time Series Evaluation ($t_{10\%}$, $t_{50\%}$& $t_{80\%}$):**

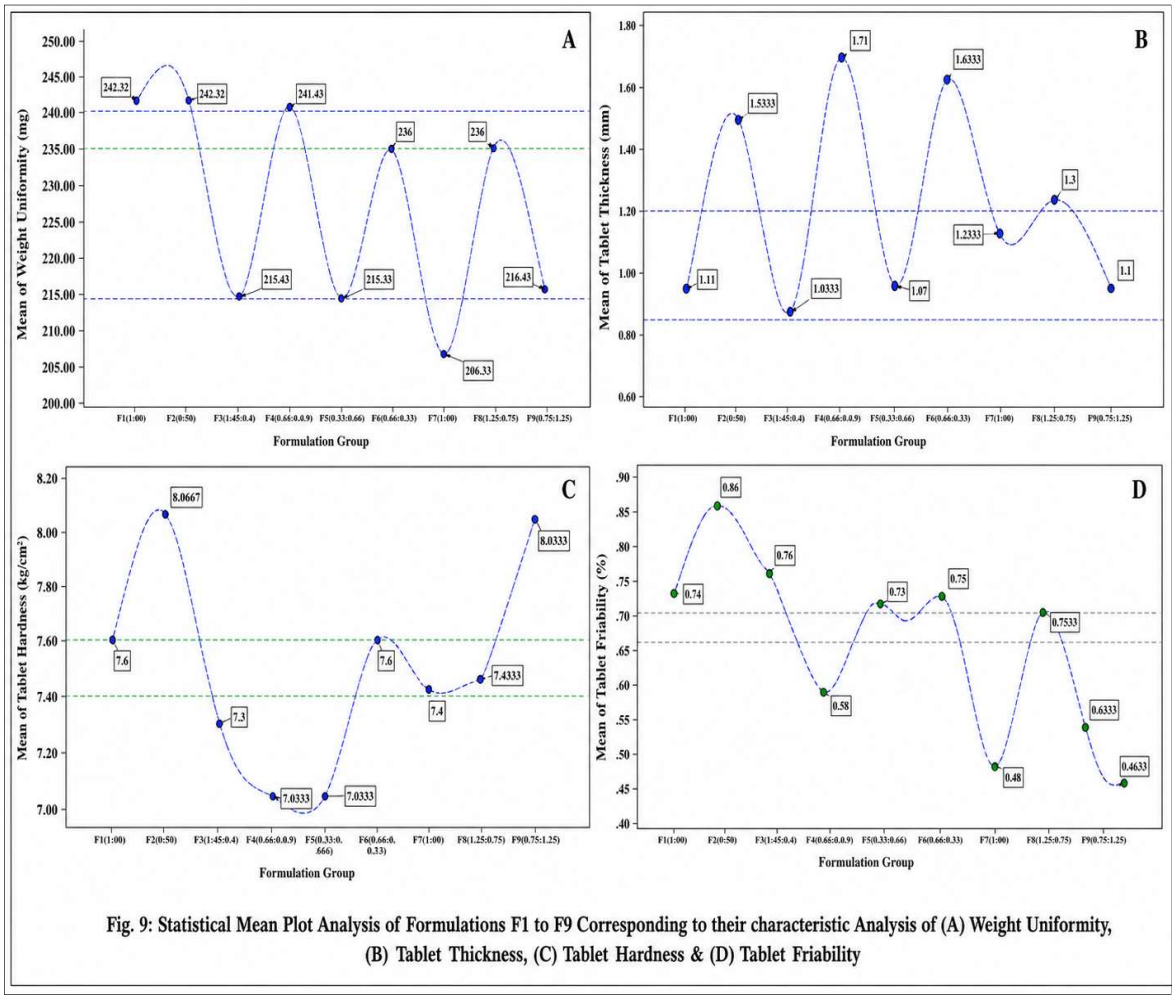


Fig. 9: Statistical Mean Plot Analysis of Formulations F1 to F9 Corresponding to their characteristic Analysis of (A) Weight Uniformity, (B) Tablet Thickness, (C) Tablet Hardness & (D) Tablet Friability

**Table 9: The distribution of mean time duration achieved by the individual formulations corresponding to their percentage release slots, i.e., t-10%, t-50%, & t-80%**

| Sl. No. | Formulation Code | Percentage (%) Release Time Interval (hr.) | | |
|---|---|---|---|---|
| | | $t_{10\%}$ | $t_{50\%}$ | $t_{80\%}$ |
| 1 | F1 | 1.36±0.037 | 5.63±0.149 | 8.84±0.279 |
| 2 | F2 | 2.29±0.020 | 5.96±0.031 | 8.7±0.064 |
| 3 | F3 | 2.43±0.018 | 5.9±0.039 | 8.5±0.062 |
| 4 | F4 | 1.94±0.500 | 5.23±0.545 | 7.7±0.579 |
| 5 | F5 | 2.70±0.055 | 6.66±0.141 | 9.63±0.205 |
| 6 | F6 | 1.08±0.057 | 4.62±0.204 | 7.27±0.326 |
| 7 | F7 | 1.49±0.030 | 5.12±0.055 | 7.84±0.096 |
| 8 | F8 | 2.11±0.042 | 5.75±0.100 | 8.48±0.144 |
| 9 | F9 | 2.54±0.094 | 6.89±0.605 | 10.15±0.989 |

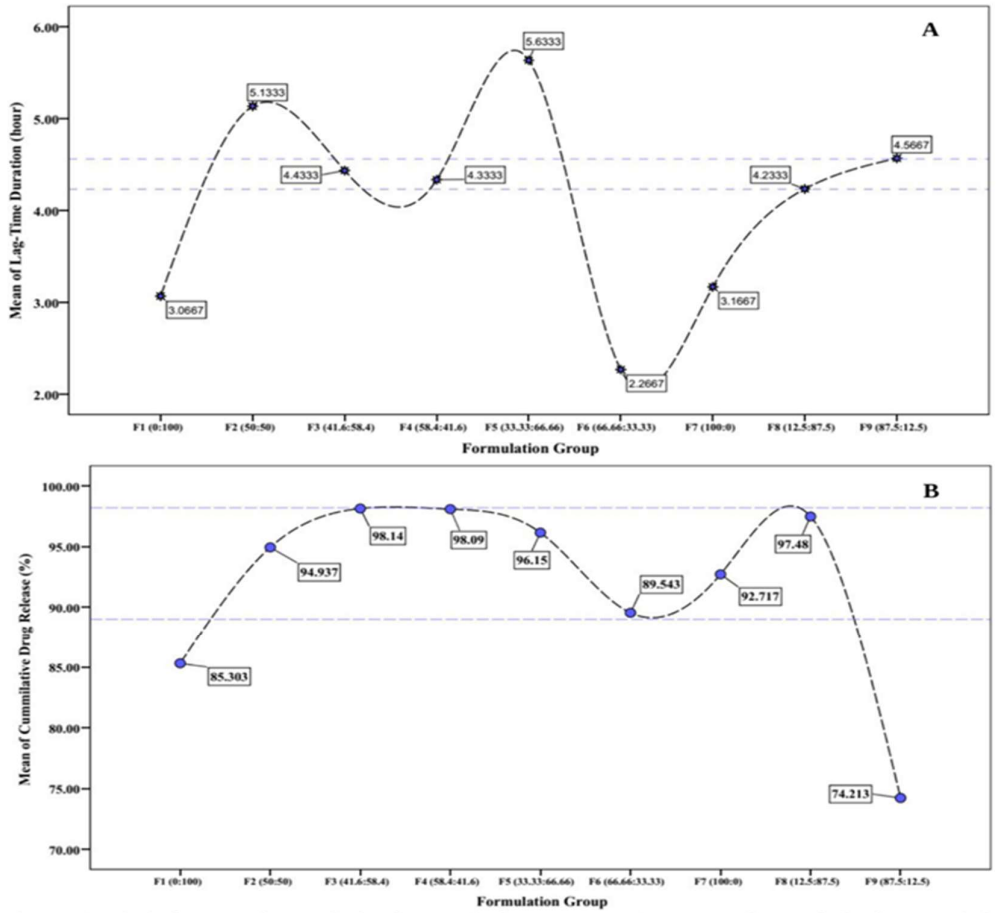


**Fig. 10: Statistical Mean Plot Analysis of Formulations F1 to F9 Corresponding to their characteristic Analysis of (A) Lag-Time Duration, (B) Cumulative % Drug Released**

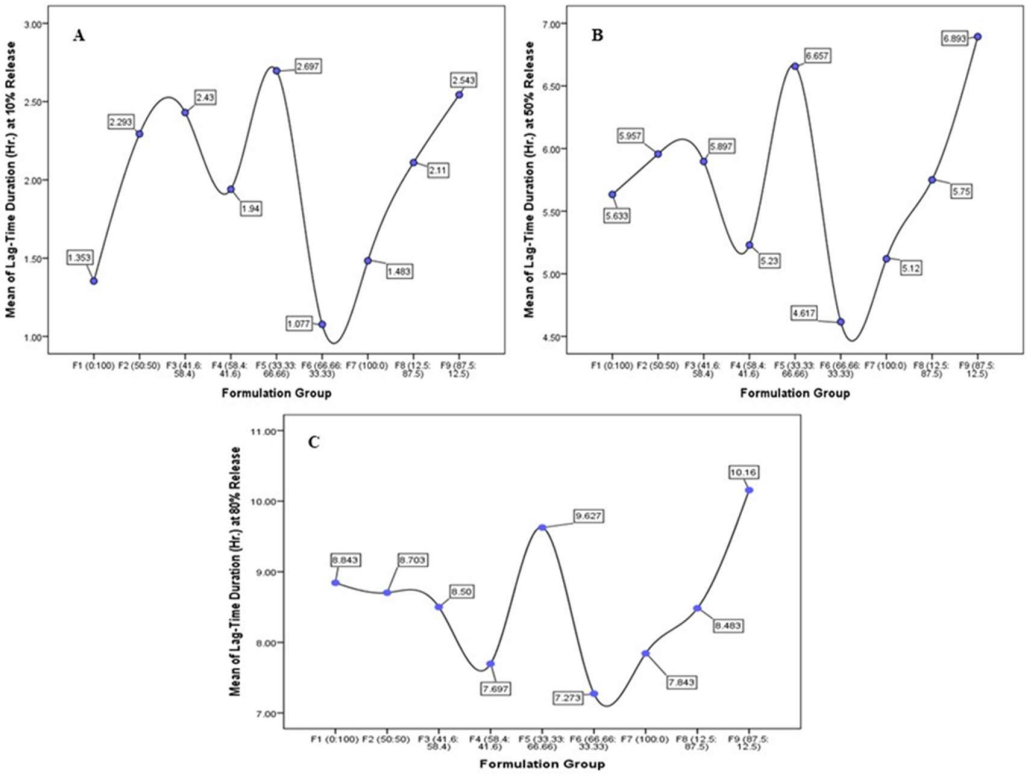


**Fig. 11: Statistical Mean Plot Analysis of Formulations F1 to F9 Corresponding to their mean time duration achieved by the individual formulations corresponding to their percentage release slots, i.e., t-10%, t-50% & t-80%**

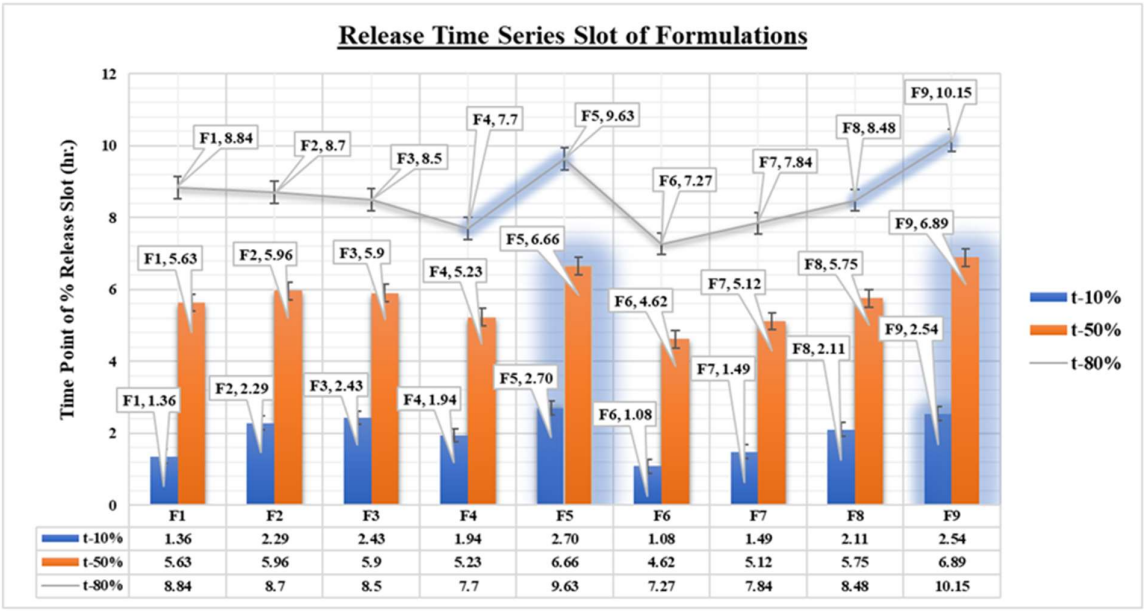


| | F1 | F2 | F3 | F4 | F5 | F6 | F7 | F8 | F9 |
|---|---|---|---|---|---|---|---|---|---|
| t-10% | 1.36 | 2.29 | 2.43 | 1.94 | 2.70 | 1.08 | 1.49 | 2.11 | 2.54 |
| t-50% | 5.63 | 5.96 | 5.9 | 5.23 | 6.66 | 4.62 | 5.12 | 5.75 | 6.89 |
| t-80% | 8.84 | 8.7 | 8.5 | 7.7 | 9.63 | 7.27 | 7.84 | 8.48 | 10.15 |

**Fig. 12: Combo-graphical presentation of different slots of release time durations, i.e., t-10%, t-50%, & t-80% of all formulations at a glance.**

## DISCUSSION

The present investigation was conceived against the backdrop of an established chronopharmacologic rationale: cardiovascular events cluster disproportionately in the early-morning hours due to a circadian surge in blood pressure, heart rate, sympathetic output, and platelet aggregation, with a concomitant decline in fibrinolytic activity [6–8]. Bedtime chronotherapy with an antihypertensive agent that suppresses this morning BP surge—such as carvedilol—has been clinically validated to flatten the 24-hour BP profile and reduce cardiovascular morbidity

[13–16]. A time-dependent, pulsatile press-coated tablet that delays carvedilol release until the pre-dawn window, therefore, represents a coherent pharmacological strategy, with the prerequisite that the lag time, post-lag burst, and kinetics all be quantitatively demonstrable in vitro.

***Pre-formulation and Analytical Characterization of Carvedilol***

The successful development of any solid dosage form rests on rigorous pre-formulation verification of drug identity and purity. The UV-visible spectrum of carvedilol in both 0.1 N HCl and pH 6.8 phosphate buffer produced a well-defined $\lambda_{max}$ at 241 nm, identical in both dissolution media (Tables 2 and 3; Figs. 1–4). This common absorption maximum confirmed the medium independence of the chromophore and provided a single, robust detection wavelength for all subsequent content uniformity, *in-vitro* dissolution, and release kinetic measurements. Crucially, Beer–Lambert linearity held over the analytical working range of 4–36 µg/ml in both media, satisfying the validation prerequisite for quantitative UV assay of the dissolution samples.

The experimentally determined melting point of 112 °C closely matches the literature value of 114 °C reported in pharmacopeial data, providing an early thermal identity confirmation of the API. ATR-FTIR spectroscopy analysis corroborated the molecular structure i.e., the characteristic absorption bands at ***3329.76 $cm^{-1}$ (N–H stretching), 2922.16 $cm^{-1}$ (C–H stretching), 1502.55 $cm^{-1}$ (C=C aromatic stretching), 1212.56 $cm^{-1}$ (C–N stretching), and 1095.50 $cm^{-1}$ (C–O bending)*** were all reproduced in the spectra of the drug–excipient physical mixtures without detectable shifting, disappearance, or new band generation (Figs. 5 and 6). The absence of new peaks is significant—any chemical interaction between carvedilol and the chosen excipients (*HPMC K100, ethyl cellulose, β-cyclodextrin, MCC, mannitol, SSG, talc, magnesium stearate*) would have manifested as band shifts or novel vibrations, which were not observed; therefore, the **drug–excipient compatibility required for a stable formulation was confirmed**.

The micromeritic properties of both pure carvedilol and the powder blend (*angle of repose 31.42°/32.14°, Carr's compressibility index 14.82%/13.84%, and Hausner's ratio 1.14/1.16*) all fell within the "good flow" range. Adequate flowability and compressibility of the pre-compression blend are essential prerequisites for uniform die-filling and reproducible tablet weight, which become especially critical in press-coated systems where the coating powder must be split into two accurately weighed halves surrounding the core.

***Core Tablet Quality Attributes***

The fast-dissolving core tablet of 6.25 mg carvedilol (incorporated as a carvedilol-β-cyclodextrin inclusion complex at 25 mg per tablet, a 1:3 drug-to-cyclodextrin ratio) was within pharmacopeial tolerance on every critical post-compression parameter. The mean weight of 130.3±2.95 mg, mean thickness of 3–3.5 mm, hardness of 4.5±0.075 kg/cm², and friability of 0.45% indicate a mechanically robust core capable not only of withstanding handling but also of resisting fracture during the press-coating compression step—a frequently neglected but practically important consideration. The short disintegration time of 210±2 sec confirms that the superdisintegrant system (sodium starch glycolate) effectively dismantles the matrix, priming the core for rapid drug liberation once the press-coat is breached. Most importantly, the drug content of ~125% (*with reference to the labelled 6.25 mg carvedilol*) is a consequence of the β-cyclodextrin complex delivering a known stoichiometric excess; this is internally consistent since only the carvedilol moiety is quantified at 241 nm and the cyclodextrin serves as a solubilizing carrier that becomes part of the molecular payload after dissolution. The complete in-vitro release of the core in pH 6.8 phosphate buffer established that the core itself is release-ready, and any retardation observed in the press-coated batches can be unambiguously attributed to the outer shell, not to the inner matrix.

***Physicochemical Characterization of Bilayer/Press-Coated Tablets (F1–F9)***

Once the core was coated with the nine HPMC K100:ethyl cellulose combinations, all batches met basic pharmaceutical quality expectations: weight uniformity stayed within ±2 mg in all formulations, thickness was reproducible within ±0.17 mm, hardness ranged from 7.03 to 8.06 kg/cm², and friability remained below the 1% pharmacopeial limit for every batch (0.64–0.86%). The friability values, in particular, confirm that direct compression of a dry blend around a preformed core can produce a mechanically durable bilayer tablet without lamination or capping—a result obtained despite markedly different polymer ratios, indicating that the press-coating technological platform is robust across the formulation space.

The Tukey-HSD post-hoc letter-overlay in Table 6 reveals, however, that weight uniformity, thickness, and hardness are highly sensitive to composition. F5 is flagged as significantly different ($P < 0.05$) from F2, F4, F6, F8, and F9 in hardness and from F2, F4, F6, and F9 in thickness. Although these differences are statistically real, all absolute values fall comfortably within pharmacopeial tolerances; therefore, these Tukey letters should be interpreted as compositional fingerprints rather than formulation failures. Crucially, F5 did not differ significantly from F1 and F3 in any of these three physicochemical parameters, and F5's friability of 0.75% sits in the middle of the range.

What truly distinguishes the batches is the cumulative percentage drug release over 8 hours, which varied from 74.22±7.16% (F9) to 98.14±1.74% (F3). **The very widespread range—from F9's incomplete 74% to F3's near-complete 98%—is a direct readout of the impact of polymer ratio on coating permeability**.

***In-vitro* Release Profiles**

The dissolution profiles of F1–F9 followed the classical sigmoidal signature expected of pulsatile press-coated systems: a flat, near-zero release phase corresponding to the lag period during which the coating resists penetration, followed by an accelerating release phase after the coating ruptures or erodes [21–24]. **F5 displayed exactly this canonical profile: slow retardation through the first 6 hours followed by sharp escalation in cumulative release to 96.15±0.70%—a value that essentially reflects "complete release" with the lowest inter-tablet variability among the moderately retarded batches**.

***Release Kinetics Modelling***

Because pulsatile delivery is mechanistically a multi-stage event (***water ingress → polymer swelling/erosion → coating rupture → diffusion-controlled core release***), no single kinetic model fits the entire curve, but model-fitting to the first 60% of release provides quantitative descriptors of the dominant transport mechanism [21]. Across all nine formulations, the Korsmeyer-Peppas model yielded the highest adjusted $R^2$ values and the lowest AIC values, confirming that drug release from these swelling/erodible press-coated matrices is best described by the Peppas power law rather than by simple diffusion, concentration-driven kinetics (first-order), or time-independent release (zero-order) [26,28].

The two formulations of central chronotherapeutic interest, F5 and F9, both achieved $R^2\_adj \approx 0.99$ (F5 = 0.9929; F9 = 0.9952), with AIC = 39.37 (MSC = 4.51) for F5 and AIC = 33.71 (MSC = 4.93) for F9. While F9's numerically tighter fit might superficially suggest a kinetic advantage, the reality is more complex: F9's n = 2.442 already indicates Super Case-II transport (relaxation-controlled, polymer-erosion-driven release), but F5's n = 4.371 is markedly higher—reflecting the more dramatic transition from a tightly held lag phase into rapid post-lag liberation, exactly the sigmoidal signature desired for chronomodulated burst delivery [22,23]. **The exponent n > 1 across all formulations classifies release as non-Fickian (anomalous) / Super Case-II, indicating that the dominant mechanism is polymer-chain relaxation and erosion rather than Fickian diffusion**, in agreement with established reports on press-coated pulsatile systems [30–32]. Both the hydrophobic EC backbone (which delays water ingress) and the high-molecular-weight swellable HPMC K100 (which subsequently dominates the rupture phase) are responsible for this n > 1 signature.

***Lag-Time Analysis and the Mechanistic Roles of EC and HPMC K100***

The principal therapeutic requirement of a bedtime-administered, time-dependent carvedilol pulsatile tablet is a lag phase long enough to survive the nocturnal dip in BP and rupture in time to deliver the drug as the morning surge begins [14,15,17–20]. The lag-time distribution at the t-10%, t-50%, and t-80% release milestones (Tables 8 and 9) is therefore the single most diagnostic dataset in this study.

*The nine formulations cluster into three behavioural groups:*

- **Short-lag formulations** (*F1, F6, F7*): F1 (HPMC:EC = 0:100, i.e., pure EC) reached $t_{10\%}$ in 1.36 hr, $t_{50\%}$ in 5.63 hr, and $t_{80\%}$ in 8.84 hr. F6 (66.66:33.33) reached these milestones in 1.08, 4.62, and 7.27 hr, respectively—the shortest lag of all formulations. F7 (pure HPMC, 100:0) took 1.49, 5.12, and 7.84 hr. The fact that both pure EC and pure HPMC produced *short* lags is mechanistically revealing: a coating composed entirely of EC, while hydrophobic, cannot swell or rupture, so dissolution medium still slowly penetrates and drug release proceeds; conversely, a coating of pure HPMC dissolves/erodes too readily. Neither extreme produces the desired delayed burst.
- **Mid-range lag formulations** (*F2, F3, F4, F8*): These four batches—with HPMC:EC ranging from 12.5:87.5 (F8) to 58.4:41.6 (F4)—produced $t_{10\%}$ values of 1.94–2.43 hr and $t_{80\%}$ values of 7.70–8.70 hr. Statistically significant differences in lag emerged, yet none of these formulations achieved the desired >6-hour delay.
- **Long-lag formulations** (*F5 and F9*): F5 (33.33:66.66) achieved $t_{10\%}$ = 2.70±0.055 hr, $t_{50\%}$ = 6.66±0.141 hr, and $t_{80\%}$ = 9.63±0.205 hr; F9 (87.5:12.5) achieved $t_{10\%}$ = 2.54±0.094 hr, $t_{50\%}$ = 6.89±0.605 hr, and $t_{80\%}$ = 10.15±0.989 hr. Both are the only formulations with $t_{50\%}$ values exceeding 6 hours—the chronotherapeutic target.

The mechanistic interpretation is now precise. EC is a hydrophobic, water-insoluble polymer that functions as a retardant by forming a continuous hydrophobic barrier that impedes the inward diffusion of dissolution medium [25,26]. It is therefore *necessary* but not *sufficient* for a long lag—a sufficiently thick EC barrier must be supplemented by a swellable/erodible mechanism that controls the rupture event. HPMC K100, a high-viscosity hydrophilic cellulose ether, swells as water penetrates, generating internal stress that ultimately ruptures the brittle EC shell and exposes the core [28,29]. F5's 33.33:66.66 ratio provides the precise balance: enough HPMC to drive a clean rupture after the lag phase, but enough EC to delay water ingress long enough for the lag. F1 (0% HPMC) lacks the rupturing mechanism; F7 (0% EC) lacks the barrier; F6 (66.66 HPMC) over-favours swelling; F9 (87.5% HPMC) over-favours erosion—an over-erosion that produces excessive retardation together with high variability.

A particularly compelling observation is the drug-release fraction at the 6-hour mark. F5 sustained only ~24% release at 6 hours—almost exactly the desired

chronobiologic profile of structural integrity during the lag, then rapid release at the target window. **By contrast, F2 released 45–50%, and F9 released 45–50% of the dose by 6 hours, meaning that they were already half-empty before the morning surge had even begun—clearly inconsistent with the chronotherapeutic intent**.

***Statistical Verification***

Post-hoc Tukey-HSD analysis (Fig. 11 and Table 6 letters) revealed that at the $t_{10\%}$ release mark, F2 and F9 did not differ significantly from F5, indicating that the early coating behaviour of these three formulations is statistically similar in the first slow-release window. However, this statistical parity at the $t_{10\%}$ mark is a superficial observation: beyond 6 hours, the cumulative release curves diverge sharply, with F5 maintaining a plateau through 6 hours before its burst, **while F2 and F9 release 45–50% prematurely**. This is exactly the chronobiologic concern flagged in the introduction that the formulation must *not* dump the dose during sleep but must hold the dose until the morning surge. **F5 alone satisfies this requirement**.

***Rationale for the Selection of Formulation F5 as the Optimal Candidate***

*A composite comparison across every characterization family confirms the choice of F5:*

- **Post-compression quality**: F5's hardness (7.03±0.06 kg/cm²) is identical to F4, statistically distinct from the highest values (F2 = 8.06, F9 = 8.03), but well within an acceptable range; friability (0.75%) is middle of the range; thickness (7.1±0.10 mm) is reproducible. The Tukey-HSD letters in Table 6 confirm F5 does not differ from F1 or F3 in thickness/hardness—two well-behaved reference formulations—so F5 is pharmacopeially compliant.
- **Cumulative release** (Table 6, Fig. 8): F5's 96.15±0.70% release over 8 hours is statistically indistinguishable from the highest-releasing batches F3 (98.14±1.74) and F8 (97.48±1.06), but the *shape* of the F5 curve is fundamentally different—the sigmoidal profile is most pronounced in F5, whereas F3's curve is more conventional and less chronobiologically targeted.
- **Lag time** (Tables 8 and 9): F5's $t_{50\%}$ of 6.66±0.141 hr is the second-longest of all formulations (F9 = 6.89±0.605 hr), with the smallest SD at $t_{50\%}$ and $t_{80\%}$ of any formulation in the long-lag group, indicating the most reproducible pulsatile behaviour.
- **Kinetics**: F5's Korsmeyer-Peppas $R^2$_adj (0.9929), AIC (39.37), MSC (4.51), and n (4.371) together describe a power-law release with strong Super Case-II transport that is more pronounced, more sigmoidal, and more reproducible than any other batch.
- **Critical-window drug retention**: F5 is the *only* long-lag formulation that releases only ~24% of its dose at the 6-hour mark, fully consistent with the chronotherapeutic requirement of suppressing—rather than exhausting—release during the nocturnal sleep window [12–16].

The comparison with F9 is the most instructive. Both ***F5 and F9*** sit in the long-lag group (>6 hr for $t_{50\%}$), and both achieve ***Korsmeyer-Peppas $R^2$_adj ≈ 0.99***. However, F9's $t_{80\%}$ lag reaches 10.15±0.989 hr with the largest standard deviation among all nine batches (0.989 hr); its cumulative release plateau at 74.22±7.16% indicates that, by 8 hours, the dose is still incompletely discharged—an over-retarded profile that defeats the quick-onset goal after lag time. F5, by contrast, terminates near-complete release (96.15±0.70%) within 9.63±0.205 hr, satisfying both the lag time and the post-lag burst requirements simultaneously. The lower EC content (66.66%) in F5 evidently produces a barrier that is more permeable than F9's (which contains only 12.5% EC in an HPMC-dominant matrix), yet F5's barrier is more mechanically robust and rupture-controllable than the purely HPMC-dominated F9 shell.

***Chronobiologic Integration***

Collectively, every result in Sections 3.1–3.4.8 converges on a single, coherent picture. Bedtime administration of carvedilol has been clinically shown to suppress the morning BP surge and reduce 24-hour mean systolic pressure when a sufficient plasma level is achieved at the surge onset [13–16]. A press-coated tablet with a ~6-hour lag, such as F5, would, if administered at bedtime (≈22:00–23:00), be positioned to begin its burst release around 04:00–05:00 and reach therapeutic plasma concentrations precisely at the circadian BP peak between 06:00 and 10:00 [4–8,10]. F5's release profile—~24% at 6 hours, escalating thereafter to ~96% by 9.63 hours—is mechanistically consistent with the chronobiology of cardiovascular risk, in which the morning surge imposes the highest demand on BP control [9,11,17,19,21–24]. The structural integrity of the EC/HPMC K100 (66.66:33.33) shell during the nocturnal dip is what allows the formulation to deliver a true pulsatile burst rather than a continuous leak [17,18,23,30–32].

**Conclusion**

Across all evaluation parameters—pre-formulation identity and purity, core-tablet quality, bilayer physicochemical characterization, dissolution behaviour, release kinetics, lag-time reproducibility, statistical significance, and chronobiologic relevance—***formulation F5 (HPMC K100: Ethyl-cellulose = 33.33:66.66)*** emerges as the ***optimal batch***. F5 simultaneously satisfied the pharmacopeial quality attributes and achieved the highest-quality Korsmeyer-Peppas fit (*$R^2$_adj = 0.9929; n = 4.371 indicating Super Case-II erosion-relaxation transport*) together with low AIC (39.37) and high MSC (4.51), and uniquely

combined an extended ~6-hour lag ($t_{50\%}$ = *6.66±0.141 hr*) with rapid, sustainable post-lag release to 96.15±0.70% in 8 hours, while retaining only ~24% of its load at the 6-hour mark—the chronobiologically critical window. ***The data therefore identify F5***, with its balanced hydrophobic EC barrier combined with a swellable HPMC K100 rupturing component, as the ***optimal press-coated pulsatile carvedilol batch*** for chronomodulated time-dependent antihypertensive therapy.

**REFERENCES**

[1] Iatridis PG. Biological Rhythms in Clinical Practice. JAMA 1990;264:3076–3076. https://doi.org/10.1001/jama.1990.03450230112048 .

[2] Garg MrS.Chronopharmacology, 2024, p. 183–9. https://doi.org/10.58532/nbennurphch20 .

[3] Reinberg A. Concepts of Circadian Chronopharmacology. Annals of the New York Academy of Sciences 1991;618:102–15. https://doi.org/10.1111/j.1749-6632.1991.tb27239.x .

[4] Setters B, Holmes HM. Hypertension in the Older Adult. Primary Care Clinics in Office Practice 2017;44:529–39. https://doi.org/10.1016/j.pop.2017.05.002 .

[5] Faraci FM, Scheer FAJL. Hypertension: Causes and Consequences of Circadian Rhythms in Blood Pressure. PubMed Central 2024;134:810–32. https://doi.org/10.1161/circresaha.124.323515 .

[6] Gaciong Z, Siński M, Lewandowski J. Blood Pressure Control and Primary Prevention of Stroke: Summary of the Recent Clinical Trial Data and Meta-Analyses. Current Hypertension Reports 2013;15:559–74. https://doi.org/10.1007/s11906-013-0401-0 .

[7] Takeda N, Maemura K. Circadian clock and vascular disease. Hypertension Research 2010;33:645–51. https://doi.org/10.1038/hr.2010.68 .

[8] Chen L, Yang G. Recent advances in circadian rhythms in cardiovascular system. Frontiers in Pharmacology 2015;6:71–71. https://doi.org/10.3389/fphar.2015.00071 .

[9] Bombelli M, Fodri D, Toso E, Macchiarulo M, Cairo M, Facchetti R, Dell'Oro R, Grassı G, Mancia G. Relationship Among Morning Blood Pressure Surge, 24-Hour Blood Pressure Variability, and Cardiovascular Outcomes in a White Population. Hypertension 2014;64:943–50. https://doi.org/10.1161/hypertensionaha.114.03675 .

[10] Turner JR, Viera AJ, Shimbo D. Ambulatory Blood Pressure Monitoring in Clinical Practice: A Review. The American Journal of Medicine 2014;128:14–20. https://doi.org/10.1016/j.amjmed.2014.07.021 .

[11] Cheng Y, Li Y, Wang J. Ambulatory blood pressure monitoring for the management of hypertension. Chinese Medical Journal 2022;135:1027–35. https://doi.org/10.1097/cm9.0000000000002028 .

[12] Kobalava Z, Troitskaya EA. Chronotherapy of hypertension: current state of the problem and prospects. Russian Journal of Cardiology 2023;28:5395–5395. https://doi.org/10.15829/1560-4071-2023-5395 .

[13] Smolensky MH, Hermida RC, Ayala DE, Tiseo R, Portaluppi F. Administration–time-dependent effects of blood pressure-lowering medications: basis for the chronotherapy of hypertension. Blood Pressure Monitoring 2010;15:173–80. https://doi.org/10.1097/mbp.0b013e32833c7308 .

[14] Cortés-Ríos J, Hermida RC, Rodriguez-Fernández M. Dosing time optimization of antihypertensive medications by including the circadian rhythm in pharmacokinetic-pharmacodynamic models. PLoS Computational Biology 2022;18. https://doi.org/10.1371/journal.pcbi.1010711 .

[15] Koga H, Hayashi J, Yamamoto M, Kitamoto K. Prevention of Morning Surge of Hypertension by the Evening Administration of Carvedilol 2005.

[16] Hermida RC, Ayala DE, Mojón A, Fernández JR. INFLUENCE OF CIRCADIAN TIME OF HYPERTENSION TREATMENT ON CARDIOVASCULAR RISK: RESULTS OF THE MAPEC STUDY. Chronobiology International 2010;27:1629–51. https://doi.org/10.3109/07420528.2010.510230 .

[17] Sarode SM, Gandhi B. A Review on Pulsatile Drug Delivery System. International Journal of Advanced Research in Science Communication and Technology 2023:121–5. https://doi.org/10.48175/ijarsct-9332 .

[18] GOMATHI J, VEERALAKSHMI B, F. FAM. PULSATILE DRUG DELIVERY: A STRATEGY FOR TREATING CHRONOTHERAPEUTIC AILMENTS. International Journal of Current Pharmaceutical Research 2023:1–8. https://doi.org/10.22159/ijcpr.2023v15i4.3012 .

[19] Pal S, Monika M, Singh M. Circadian rhythms regulated pulsatile drug delivery system. International Journal of Health Sciences 2022:7944–65. https://doi.org/10.53730/ijhs.v6ns4.10374 .

[20] Ismail Y, Voleti VK, Priya S. Chronotherapy and Pulsatile Drug Delivery Systems: Aligning Pharmacotherapy with Circadian Rhythms, 2026, p. 39–48. https://doi.org/10.9734/bpi/psnid/v10/7019 .

[21] Shidhaye S, Lotlikar V, Ghule A, Phutane P, Kadam V. Pulsatile delivery systems: An approach for chronotherapeutic diseases. Systematic

Reviews in Pharmacy 2010;1:55–55. https://doi.org/10.4103/0975-8453.59513 .
[22] Ali J, Ahuja A, Baboota S, Qureshi J, Arora S. Pulsatile drug delivery systems: An approach for controlled drug delivery. Indian Journal of Pharmaceutical Sciences 2006;68:295–295. https://doi.org/10.4103/0250-474x.26655 .
[23] Sharma N, Saini PK, Mishra C, Sharma C. Pulsatile drug delivery: Advances, mechanisms and future perspectives. International Journal of Pharmacy and Pharmaceutical Science 2025;7:229–32. https://doi.org/10.33545/26647222.2025.v7.i2c.215 .
[24] Parmar RD, Parikh RK, Vidyasagar G, Patel D, Patel CJ, Patel BD. Pulsatile Drug Delivery Systems: An Overview. International Journal of Pharmaceutical Sciences and Nanotechnology 2009;2:605–14. https://doi.org/10.37285/ijpsn.2009.2.3.3 .
[25] Benzine Y. Enzymatically triggered polymeric drug delivery systems for colon targeting. HAL (Le Centre pour la Communication ScientifiqueDirecte) 2019.
[26] Jan MS, Alam W, Shabnam M. Fundamentals Applications of Controlled Release Drug Delivery. Pharmaceutical science., 2023. https://doi.org/10.5772/intechopen.113283 .
[27] Yoshida T, Lai TC, Kwon GS, Sako K. pH- and ion-sensitive polymers for drug delivery. Expert Opinion on Drug Delivery 2013;10:1497–513. https://doi.org/10.1517/17425247.2013.821978 .
[28] Madan HS. Polymer in Pharmaceutical Drug Delivery System. International Journal for Research in Applied Science and Engineering Technology 2021;9:1552–8. https://doi.org/10.22214/ijraset.2021.39568 .
[29] Chowdary KPR, Rao YS. Mucoadhesive Microspheres for Controlled Drug Delivery. Biological and Pharmaceutical Bulletin 2004;27:1717–24. https://doi.org/10.1248/bpb.27.1717 .
[30] Toshib ASM. Development And Evaluation Of Pressed Coated Floting Pulsatile Tablet Of Atenolol. Zenodo (CERN European Organization for Nuclear Research) 2023. https://doi.org/10.5281/zenodo.8396445 .
[31] Shrivastava A. PULSATILE DRUG DELIVERY SYSTEMS: A CASE OF BETA-BLOCKERS. Asian Journal of Pharmaceutical and Clinical Research 2019:16–22. https://doi.org/10.22159/ajpcr.2019.v12i3.29704 .
[32] Damanhuri D. Penagaruhkompentensiprofesionalisme guru studifiqihterhadapminatbelajarsiswa di mts sa'adatuddarain Jakarta Selatan. AAPS PharmSciTech 2002;5. https://doi.org/10.1208/pt050454 .
[33] El-Say KM, Hosny KM. Optimization of carvedilol solid lipid nanoparticles: An approach to control the release and enhance the oral bioavailability on rabbits. PLoS ONE 2018;13. https://doi.org/10.1371/journal.pone.0203405 .
[34] Anjani QK, Sabri AHB, McGuckin MB, Li H, Hamid KA, Donnelly RF. In Vitro Permeation Studies on Carvedilol Containing Dissolving Microarray Patches Quantified Using a Rapid and Simple HPLC-UV Analytical Method. AAPS PharmSciTech2022;23:273–273. https://doi.org/10.1208/s12249-022-02422-6 .
[35] Meravanige G, Gajula LR, Rangappa AB, Goudanavar P, Sridhar SK, Naveen NR, Sreeharsha N, Shiroorkar PN, Asif AH, Telsang M. Optimization and Characterization of Lamivudine-Loaded TCS-PEG/MMT Polymeric Nanocomposites for Enhanced Antiretroviral Therapy. Indian Journal of Pharmaceutical Education and Research 2024;58. https://doi.org/10.5530/ijper.58.3s.92 .
[36] Kumar I, Chaudhary D, Thakur B, Pandit V. Formulation and Evaluation of Piroxicam Fast Dissolving Tablets Using Direct Compression and Sublimation Method. Journal of Drug Delivery and Therapeutics 2020;10:17–25. https://doi.org/10.22270/jddt.v10i3-s.4063 .
[37] Mahapatra APK, Saraswat R, Botre M, Paul B, Prasad N. Application of response surface methodology (RSM) in statistical optimization and pharmaceutical characterization of a patient compliance effervescent tablet formulation of an antiepileptic drug levetiracetam. Future Journal of Pharmaceutical Sciences 2020;6. https://doi.org/10.1186/s43094-020-00096-0 .
[38] García MC, Manzo RH, Jimenez-Kairuz AF. Polysaccharides-based multiparticulatedinterpolyelectrolyte complexes for controlled benznidazole release. International Journal of Pharmaceutics 2018;545:366–77. https://doi.org/10.1016/j.ijpharm.2018.05.017 .
[39] Xu Y, Wang Y, Li C, Han T, Chen H, Chen W, Zhong Q, Pei J, Haenen GRMM, Li Z, Moalin M, Zhang M, Chen W. Preparation, characterization, and biological activity of the inclusion complex of dihydroquercetin and β-Cyclodextrin. AAPS Open 2023;9. https://doi.org/10.1186/s41120-023-00083-8 .
[40] Vukomanović M, Gazvoda L, Kurtjak M, Hreščak J, Jaklic B, Moya-Andérico L, Cendra M del M, Torrents E. Development of a ternary cyclodextrin–arginine–ciprofloxacin antimicrobial complex with enhanced stability. Communications Biology 2022;5:1234–1234. https://doi.org/10.1038/s42003-022-04197-9 .
[41] Saoji SD, Raut NA, Dhore PW, Borkar CD, Popielarczyk M, Dave VS. Preparation and Evaluation of Phospholipid-Based Complex of Standardized Centella Extract (SCE) for the Enhanced Delivery of Phytoconstituents. The

AAPS Journal 2015;18:102–14. https://doi.org/10.1208/s12248-015-9837-2 .
[42] Wang Y, Wen S, Zhao Y, Gui L, Mou Y, Wang D. New polymorph of tofacitinib citrate and in vitro equivalence study of its sustained-release tablets. PLoS ONE 2025;20. https://doi.org/10.1371/journal.pone.0332664 .
[43] Kamil MM, Bayoumi AA. Co-Milling: A Successful Approach to Enhance Solubility of a Poorly Soluble Antihypertensive Drug. INDONESIAN JOURNAL OF PHARMACY 2023. https://doi.org/10.22146/ijp.7072 .
[44] Aleti R, Murthy KVR. Development and characterization of chronotherapeutic tablets of sacubitril-valsartan supramolecular complex using hupu gum and lannea gum by compression coating. Journal of Applied Pharmaceutical Science 2023. https://doi.org/10.7324/japs.2023.120714 .
[45] Maurya H, Kumar T. FORMULATION, STANDARDIZATION, AND EVALUATION OF POLYHERBAL DISPERSIBLE TABLET. International Journal of Applied Pharmaceutics 2019;11:158–158. https://doi.org/10.22159/ijap.2019v11i1.30113 .
[46] Hossain MdS, Hossain MA, Anisuzzman Md. FORMULATION DEVELOPMENT AND EVALUATION OF CARVEDILOL TABLET. International Research Journal of Pharmacy 2013;4:96–100. https://doi.org/10.7897/2230-8407.04816 .
[47] Uboldi M, Gelain A, Buratti G, Gazzaniga A, Melocchi A, Zema L. Development of 4D printed intravesical drug delivery systems: Scale-up of film coating. ArchivioIstituzionale Della Ricerca (UniversitaDegliStudi Di Milano) 2023;87:104875–104875. https://doi.org/10.1016/j.jddst.2023.104875 .
[48] Kotadiya RM, Savant NP, Upadhyay UM. 10.51847/9edBABN. Time to Knit 2000. https://doi.org/10.51847/9edbabn .
[49] Ghimire P, Shrestha AC, Sandhya P, Bidur C, Samir D. Pharmacopoeial comparison of in-process and finished product quality control test for pharmaceutical tablets. GSC Biological and Pharmaceutical Sciences 2020;11:155–65. https://doi.org/10.30574/gscbps.2020.11.3.0174 .
[50] Patel SG, Siddaiah M. Formulation and evaluation of effervescent tablets: a review. Journal of Drug Delivery and Therapeutics 2018;8:296–303. https://doi.org/10.22270/jddt.v8i6.2021 .
[51] Barde L, Suruse PB, AGRAWAL S, Kalkotwar RS, Sable V, Tare H. DESIGN, DEVELOPMENT AND FABRICATION OF MOUTH-DISSOLVING TABLETS CONTAINING EXTRACT OF TRIBULUS TERRESTRIS FOR THE TREATMENT OF HYPERTENSION. International Journal of Applied Pharmaceutics 2023:234–41. https://doi.org/10.22159/ijap.2023v15i3.47662 .
[52] CHANDARANA DA, Patel KS, PATEL SC, Patel DR, Prajapati S. FORMULATION AND EVALUATION OF MUCOADHESIVE BUCCAL TABLETS OF CARVEDILOL. International Journal of Applied Pharmaceutics 2020:170–81. https://doi.org/10.22159/ijap.2020v12i4.37849 .
[53] Shankar KR, Aminabee S, Lakshmi KNVC, REDDY GR, Shaik R, TIYAGURA V, Sultana SA, Basha SS, SAI KM, BHAGAVAN J, KUMAR CD. EFFECT OF VARIOUS SUSTAINED RELEASE POLYMERS ON FLOATING TABLETS OF CARVEDILOL PHOSPHATE-A COMPARATIVE STUDY. International Journal of Applied Pharmaceutics 2023:125–31. https://doi.org/10.22159/ijap.2023v15i6.49170 .
[54] Ahmad NR, Rahman GN. Novel Ultrasensitive Eco-Friendly Spectrophotometric Determination of Carvedilol in Pharmaceutical Preparations and Environmental Wastewater Samples: Application to Content Uniformity Testing. Journal of Gastroenterology & Hepatology Reports 2025:1–4. https://doi.org/10.47363/jghr/2025(6)178 .
[55] Hamed R, Awadallah A, Sunoqrot S, Tarawneh O, Nazzal S, AlBaraghthi T, Sayyad JA, Abbas A. pH-Dependent Solubility and Dissolution Behavior of Carvedilol—Case Example of a Weakly Basic BCS Class II Drug. AAPS PharmSciTech2015;17:418–26. https://doi.org/10.1208/s12249-015-0365-2 .
[56] Yamsani VV, Gannu R, Kolli C, Mutheneni SR, Yamsani MR. Development and in vitro evaluation of buccoadhesive carvedilol tablets. Acta Pharmaceutica2007;57:185–97. https://doi.org/10.2478/v10007-007-0015-7